Dissertation for the degree of Doctor of Philosophy

Control strategy against ripe rot on the kiwifruit caused by *Botryosphaeria dothidea* in storage

Yong Ho Shin

Department of Agriculture
The Graduate School
Jeju National University

February 2024

Control strategy against ripe rot on the kiwifruit caused by *Botryosphaeria dothidea* in storage

A Dissertation submitted to the graduate school of
Jeju National University in partial fulfillment of
the requirements for the degree of Doctor of
Philosophy in Agriculture
under the supervision of **Professor Yong Chull Jeun**

The dissertation for the degree of Doctor of Philosophy
by **Yong Ho Shin**
has been approved by the dissertation committee.

December 2023

Chair	Prof. Dong Soon Kim	
Member	Prof. Hyo Yeon Lee	
Member	Prof. Kwan Jeong Song	
Member	Prof. Yong Suk Chung	
Thesis Director	Prof. Yong Chull Jeun	

CONTENTS

Part A. Field study of ripe rot infection

Part B. Genetic control in kiwifruit against ripe rot

Part C. Chemical control of kiwifruit against ripe rot

Part A. Field study of ripe rot infection

List of Figures

List of Tables

ABSTRACT

Ripe rot on kiwifruit caused by *Botryosphaeria dothidea* has been severed recently in the kiwi orchards in Jeju. In this study, in order to protect the kiwifruit from the disease effectively, current pathogen infection frequency and disease infection activated period were investigated. To know infection frequency by ripe rot, 86 kiwi fruits were collected and identified. Also, the kiwifruits from two orchards were sealed on different 11 periods during cultivation and counted infected kiwi fruit after harvest during storage season for window infection. In the result of disease infection frequency check test, 76 % of kiwifruits shown the disease symptoms were identified as *B. dothidea*. In the window infection, most of kiwi fruits were infected during fruitset to late June period. Basis on these results, most of postharvest disease was caused by *B. dothidea* and it was suggested that efficient control treatment should be carried out during May to June.

Key words: control key time, field infection, kiwi disease, ripe rot distribution

I. INTRODUCTION

Kiwifruits contain more than 70 species, among them two different color types of the fruits were mainly cultivated as commercial products; green flesh kiwifruit (*Actinidia deliciosa*), and yellow flesh kiwifruit (*Actinidia chinensis*) (Ferguson, 2011; Kim et al., 2020). In Korea, green flesh kiwifruit cultivar such as Hayward (*Actinidia deliciosa* var. *deliciosa*) was cultivated from 1970, and gold flesh kiwifruit Hort16A (*A. chinensis* var. *chinensis* cultivar 'Hort16A') was cultivated from 2004 (Ciacci et al., 2013; Lee et al., 2020; Kim and Ko, 2018a). Kiwi production of green flesh kiwifruit was 65 % and yellow flesh kiwifruit was 33% in 2017 and yellow flesh kiwifruit would be more competitive leading cultivating area expansion (Kim et al., 2017).

Kiwifruit contains lots of nutrition as fat, carbohydrates, protein, vitamin A, B, C, E, K, minerals, flavonoid, polyphenols, chlorophyll, inositol, lutein and carotenoid assisting human's healthy maintenance such as prevention of depression, anemia, cancer oxidation effect, and inflammatory effects (Graziani et al., 2017; Latocha et al., 2010; Suksomboon et al., 2019; Tyagi et al., 2015; Yang et al., 2019; Richardson et al., 2018; Boland et al., 2013; Singletary, 2012;). Because of beneficial effect of kiwifruits, the kiwi global production has been increased steadily to approximately 4.35 million tons in 2016, and domestic kiwifruit consumption was kept increasing similarly (Wang et al., 2021a; Kwack et al., 2022; Kim et al., 2023; Deng et al., 2023). Correspondingly kiwi cultivating area in Korea was 1300 ha focusing on south part of Korea near ocean including Jeju which was the largest producing area taken at 44% of kiwi production (Kim et al., 2017; Kwack, 2022; Ko et al., 2016).

However, kiwifruit industry has damaged by bacteria canker disease caused by

Pseudomonas syringae pv. *actinidiae* (*Psa*) from 1988 in Korea (Koh and lee, 1992). Especially, *Psa* biovar 3 which have high pathogenicity to the kiwifruit was reported first in Jeju on 2011 and outbreak severely in commercial cultivar Hort16A introduced from Newzealnd (Koh et al., 2017). Therefore, new variety of yellow flesh kiwifruit (*A. chinensis* var. *chinensis* cultivar 'Gold3') having high resistant against *Psa* was introduced to Korea (Donati et al., 2014; Ledesma et al., 2021; Koh et al., 2017).

The new variety Gold3 kiwifruit has resistance to *Psa*, but ripe rot has threatened on Gold3 kiwifruit farm contracted with Zespri in Jeju Island Korea Recently. Crop loss caused by this disease has reported other cultivar and the amount of the loss is increasing in Korea every year (Kim and Koh, 2018b; Koh et al., 2005). The causal pathogenic fungus has been known as *Botryosphaeria dothidea* on Gold3 kiwifruit in the previous study (Ledesma et al. 2021). The fungus is endemic to Asia, the United States, Europe, and Australia and can therefore be considered a worldwide threat of kiwifruit production (Ren et al., 2022; Zhou et al., 2015, Zhang et al., 2019). In this reason, rapid control method should be prepared on Gold3 kiwifruit against *B. dothidea.*

In a prior study focusing on direct applicate by growers (Ledesma, 2020), it was observed that the ripe rot pathogen could directly penetrate the kiwifruit cell wall, and severe disease symptom was shown when the fruit was wounded and inoculated. Also, ripe rot pathogen could infect the other kiwi cultivars such as Hayward, and Hort16A. However, those previous studies were carried out under artificial condition focusing on cultural control the ripe rot. Moreover, the recent introduction of the Gold3 variety to Korea implies a scarcity of information concerning *B. dothidea* in association with Gold3. Hence, the development of diverse control strategies involving chemical or genetic methods was essential. Gathering fundamental information, such as the isolation proportion and infection period of *B. dothidea*, would be important for control the ripe rot.

In these researches, to reveal the distribution of *B. dothidea* on the kiwifruits,

pathogens were isolated from infected kiwifruit shown ripe rot. Also, potential window of infection was investigated in order to try and understand if there are key times of *B. dothidea* infection during cultivating period.

II. MATERIALS AND METHODS

1. Miscellaneous isolations

A. Morphological analysis

Fruits showing ripe rot from a range of orchards were sent for isolation and identification In order to further elucidate the causal agent. In total 86 fruits were provided from 10 different orchards with samples either collected in the field or in the packinghouse during packing. For isolation of fungal pathogen, the surface of fruit was sterilized by immersion with 1% sodium hypochlorite and 70% ethanol, then air dried. The site showing disease symptom was cut ca. 1 cm^2 in size with a sterile scalpel. Four pieces of epidermis of the fruit were placed onto potato dextrose agar (PDA). The plates were incubated at 28℃ for 3 days. All isolations showing fungal growth were sub-cultured to an oat meal agar (OMA) medium at 28℃ under light with aerobic condition for 7 days. For sporulation, fungi grown on OMA were rubbed with loop and incubated same condition for 7days. Characteristic of conidia was reported as cellular, hyaline, 17- 22 µm in length and rounded ends (Marsberg et al., 2017). The pycnidium and conidia were observed with a light microscope (BX60, Olympus, Tokyo, Japan).

1. Miscellaneous isolations

B. Molecular analysis

To do DNA extraction, isolated fungi from infected kiwifruits were re-cultured in potato dextrose broth media (PDB) in shaking incubator at 28℃ and 80 rpm for 3 days. The fungal mass in PDB was carried out the DNA extraction using CTAB methods (Aamir et al., 2015). Genomic DNA was amplified with conventional PCR using ITS1 (TCCGTAGGTGAACCTGCGG) and ITS4 primers (TCCTCCGCTTATTGATATGC) targeting internal transcribed space in 18s ribosomal RNA at 581 bp for amplicon. PCR products were carried out sequencing service from molecular analysis company Macrogene (Seoul, Korea) and compared sequence using blast service in National Center for Biotechnology Information (NCBI) site. The sequences of nucleotides were analyzed with generating phylogenetic tree using neighbor-joining analyses of 1000 bootstraps with the MEGA software program (Ver. 11.0.13) (Saitou and Nei, 1987). Total 11 isolates were selected showing different mycelia growth on PDA from 65 fungi for the phylogenetic tree analysis. Original gene of 18s ribosomal RNA sequence information of *B. dothidea*, *Diaporthe nobilis*, and *Diaporthe phaseolorum* for base data of the tree was acquired from NCBI site.

2. Window infection

A. treatment in orchard

Two Gold3 orchards in greenhouse with a known history of ripe rots in Jeju were chosen for this experiment. A total 4,400 fruitlets (2,200 each orchard) were bagged immediately after fruit-set on May. The kiwifruit was exposed for 2 or 4 weeks by bagging off and on at the different time schedule. As negative control kiwifruit bagged whole time were used and as positive control not bagged kiwifruit were used (Table 1).

Each orchard 200 kiwifruit were replicated per treatment. Fruit was harvested from the treated area before commercial harvest and immediately assessed for any ripe symptom development. The asymptomatic kiwifruit were stored at 4 ℃ until assessment of disease occurrence. Assessment was fortnightly carried out and any fruit showing ripe rots symptoms were recorded. Fungi were isolated from the 10 symptomatic fruit each fortnight form the storage and the fungal isolates were identified by morphological diagnosis.

Table 1. Time schedule of bags on and off in two different Gold3 orchards in Jeju on 2022

Period of expose	Date of bags (day/month)			
	KPIN 4538		KPIN 8338	
	off	on	off	on
Immediately after fruitset to Early-June	18/5	3/6	19/5	3/6
Early-June to mid-June	3/6	16/6	3/6	16/6
Mid-June to late-June	16/6	30/6	16/6	30/6
Late-June to mid-July	30/6	14/7	30/6	14/7
Mid-July to late-July	14/7	29/7	14/7	29/7
Late-July to late-August	29/7	25/8	29/7	25/8
Late-August to late-September	25/8	22/9	25/8	22/9
Late-September to mid-October	22/9	13/10	22/9	14/10
Early-October to mid-October	5/10	13/10	5/10	14/10
Bagged whole time (negative control)	Not required	18/5	Not required	19/5
Not bagged at all (positive control)	Not required	Not required	Not required	Not required

2. Window infection

B. Fungal isolation and identification

Surface of the fruit was sterilized with 1% sodium hypochlorite for 60s and in 70% ethanol for 60s and then air dried. The inoculation site was cut in the shape of a "V" and peeling back ca. 1 cm^2 of the epidermis tissue with a sterile scalpel. Two small pieces from the outer pericarp of the fruit under the skin's external symptom were placed onto potato dextrose agar (PDA) medium (Sigma Aldrich, Inc., St. Louis, Missouri, United States). The plates were incubated at 25℃ for 7 days.

To sporulation, the fungal isolates were transferred in oatmeal agar medium at 25℃. At 7 days after incubation, the hyphae on the medium were rubbed with a loop and incubated at 28℃ under light for another 7 days. The fungal conidia were observed under an optical microscope with bright field filter condition (Leica DM750 Microsystems, Wetzlar, Germany).

III. RESULTS

1. Miscellaneous isolation

Mycelium of fungi was isolated from all symptoms showing ripe rot on the kiwifruits and conidia were compared for identification of the isolated fungi. PDA was covered with mycelia of *B. dothidea* as full size at 3days after inoculation (Fig. 1A) and the mycelia formed black pigment at 7 days after inoculation (Fig. 1B). After rubbing the mycelia on OMA, pycnidia and conidia were formed (Fig. 1C-D). Most of fungi formed spores which were morphologically identified as *B. dothidea* to 76% (Table 2). However, some fungi did not form spores or could not be identified to 24%. Whilst this provides further evidence to support that *B. dothidea* is the causal agent of ripe rot there were 2 of the 10 orchards that predominately had another fungus present which warrants further investigation.

In results of molecular analysis, 9 fungi were identified as *Botryosphaeria dothidea*, and two fungi were identified as *Diaporthe nobilis* and *Diaporthe phaseorlorum*. In the phylogenetic tree, 9 fungi shown similar growth phase had high percent of relationship with *Botryosphaeria dothidea* 18 s ribosomal RNA gene from NCBI, whereas other 2 fungi were separated as different branch (Fig. 2).

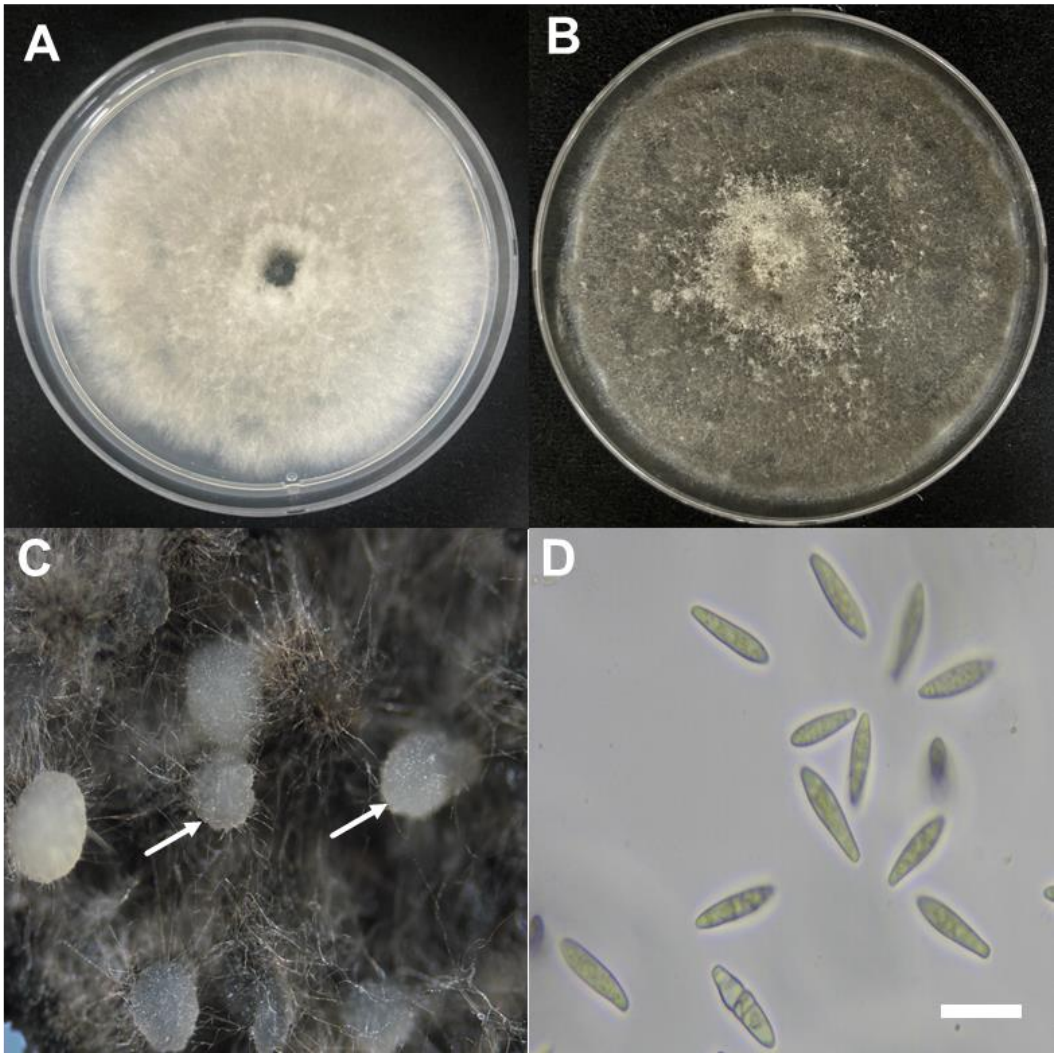

Figure 1. Mycelia growth on PDA media at 3days after inoculation (A), on oatmeal agar media at 14 days after inoculation (B), pycnidia (C), and conidia (D) observed with an optical microscope. The arrow indicates pycnidia of *B. dothidea*. The bar indicates 10μm.

Table 2. Number of kiwifruits from which *B. dothidea* was isolated on the symptom showing ripe rot collected in the various orchards in Jeju.

Variety of kiwifruit	Orchard code	Total number of fruits tested	Number of fruits *B. dothidea* isolated	Number of fruits without *B. dothidea* fungi
Gold3	46010MA1	7	6	1
	30500MA1	6	6	0
	2566MA1	10	8	2
	14590MA1	8	6	2
	17190MA1	5	1	4
	57370MA1	10	10	0
	94931MA1	10	8	2
	72900MA1	10	9	1
	21680MA1	10	7	3
	1044MA2	10	4	6
	Total number of fruit	86	65	19
	Total (%)		76	24

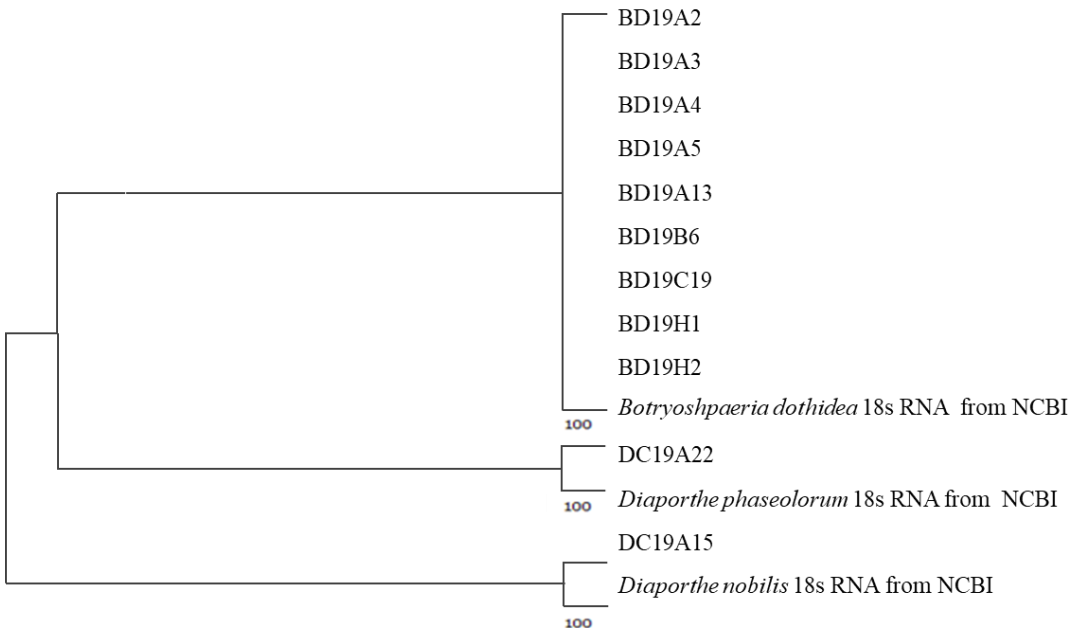

Figure 2. Phylogenetic tree of the 18s ribosomal RNA gene of pathogens isolated from kiwifruit infected with ripe rot, and 18s ribosomal RNA gene of *Botryosphaeria dothidea*, *Diaporthe phaseorlorum*, and *Diaporthe nobilis* from NCBI site. The number on branches represents the percentage of 1,000 bootstrap replicates. The tree was generated using neighbor-joining analysis.

2. Window infection

Fungal hyphae were isolated from the kiwifruit showing ripe rot or any symptoms. Among the isolates some fungi produced conidia on oatmeal medium which were identified as *B. dothidea* by morphological observation. In this experiment some of conidia were identic with those of *B. dothidea* (Fig. 1). The other fungal isolates could not identify which did not form any conidia (Data not shown). Lots of kiwifruit were infected either by *B. dothidea* or by unidentified pathogen when the fruit were not bagged in whole cultivation period. About 55% and 34% of fruit were symptomatic in Mr. Kim orchard KPIN 4538 and in Mrs. Kim KPIN 8338 orchard, respectively. Also, about 23% and 10% were infected by *B. dothidea* at each orchard, respectively (Table 3).

However, the bagged fruit in whole period were rarely infected either by *B. dothidea* or by unidentified pathogen (Table 3). These results indicated that pathogen including *B. dothidea* could not contact with kiwifruit by blocking with bagging pack. Similarly, just a few of exposed fruit form late-June to mid-October were symptomatic (Table 3).

More number of fruit were infected when they were exposed for 2 weeks during the period from immediately after fruitset to late-June (Table 3). These more infection was observed in both orchards. It is not clear why the kiwifruit exposed in the period were more susceptible to infection. However, in the previous experiment similar results have been derived in which infected fruit were found when they were exposed between May to June

(Jeun, 2019). Therefore, it was suggested that protection activity in the period of May to June might be effective than doing in other time schedule.

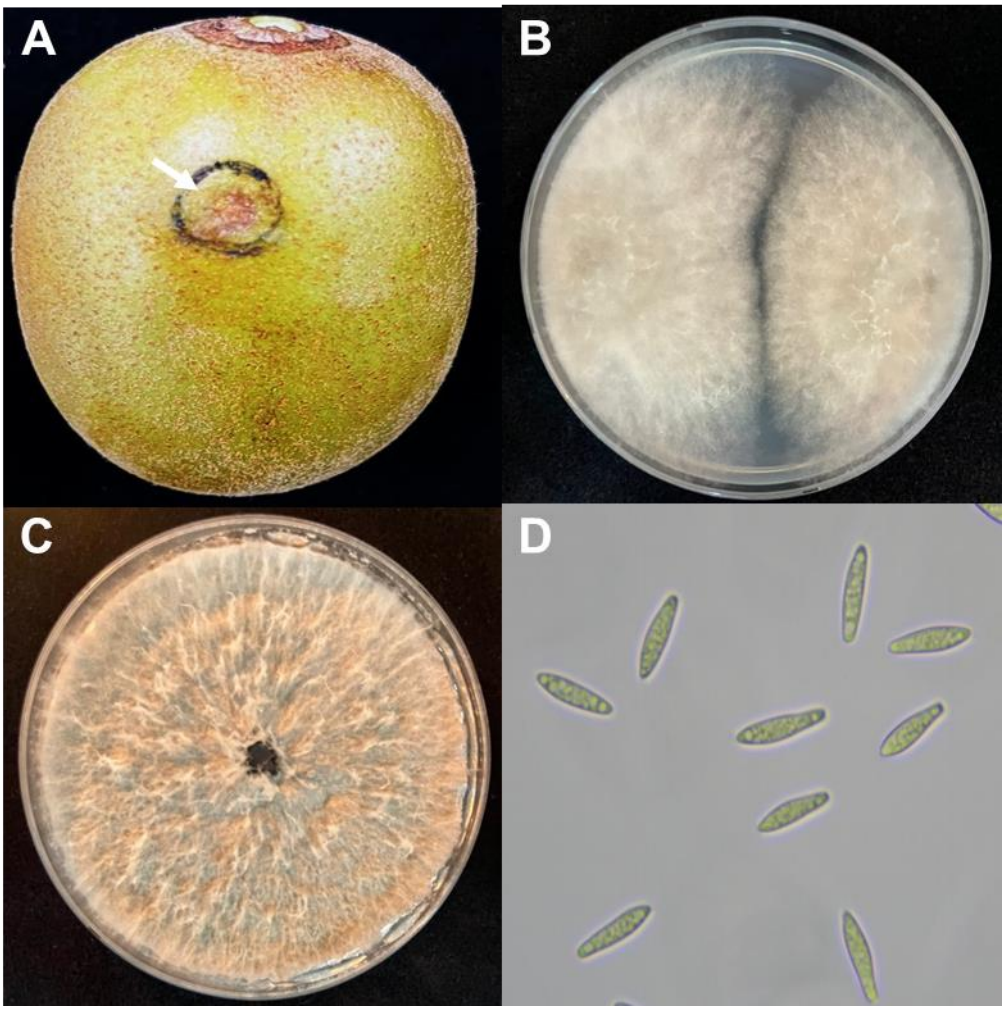

Figure 3. Symptom of ripe rot infected kiwi fruit (A), PDA *medium* isolated with flesh tissue shown ripe rot symptom (B), sub-culture from isolated Oatmeal agar media (C), and conidia observed with an optical microscope (D).

Table 3. Number of kiwifruit infected by *B. dothidea* or by unidentified pathogen after treatment with different bagged period of kiwifruit in two different orchards

Period of expose	Number of fruits infected by *B. dothidea* / Number of total fruits	
	KPIN 4538	KPIN 8338
Immediately after fruitset to Early-June	4/192	11(15)*/189
Early-June to mid-June	3(5)/187	8(11)/182
Mid-June to late-June	4(4)/183	13(28)/177
Late-June to mid-July	0(0)/189	0(0)/182
Mid-July to late-July	1(1)/168	1(1)/176
Late-July to late-August	0(1)184	1(1)/188
Late-August to late-September	1(1)/181	2(3)/182
Late-September to mid-October	1(2)/184	0(0)/169
Early-October to mid-October	1(1)/187	0(0)/163
Bagged whole time	1(1)/190	2(2)/186
Not bagged at all	23(76)/180	18(46)/187

* Number in the parentheses indicates fruits infected by unidentified pathogen

IV. DISCUSSION

Kiwifruit industry in Jeju was damaged severely by ripe rot caused by *Botryosphaeria dothidea*. It already reported that the pathogen could infect various kiwifruit such as green flesh, yellow flesh, and red flesh kiwifruits. Among them, yellow and red flesh kiwifruit could be infected by postharvest disease because of their high sugar contents compared to green flesh kiwifruit (Kim and Koh, 2018c). Kiwifruit variety Gold3 used in this study would be infected by ripe rot severely because the species was gold flesh kiwifruit. In this research, 72 fruits would be infected by fungal pathogens in 86 kiwifruits showing rot symptom (data not shown).

There were some of reports about isolation the postharvest disease pathogens from the other species. First report of kiwifruit ripe rot caused by *B. dothidea* in Korea was green flesh kiwifruit Hayward (*Actinidia deliciosa* var. *deliciosa*) on 1999, that 83.3% of *B. dothidea* was isolated from postharvest disease (Koh et al., 2003; Koh et al., 2005). Also, other yellow flesh kiwifruit varieties bred in Korea, Hallagold, Jecygold, and Jecysweet were shown high percent of *B. dothidea* infection rate at 100%, 87.5%, and 96.4 % respectively (Kwon et al., 2011). In this research, isolated rate of *B. dothidea* was 76% from infected kiwifruits (Table 2), and *B. dothidea* was 90% from isolated fungal group (data not shown) indicating that *B. dothidea* was main causal pathogen of postharvest disease showing rot symptom.

To control the ripe rot pathogen *B. dothidea*, life cycle as infection timing is important. The pathogen could be overwintering in kiwi orchards and infects kiwifruit on May after fruits set (Zhou et al., 2015). Also, the pathogen was known infection targeting the

leaves, stem, and shoot (Nazerian et al., 2019; Wang et al., 2021b). However, even the pathogen infected kiwifruit on May ripe rot symptom could not be observed until harvest season and the ripe rot symptom was expressed severely on storage season at 12 weeks after harvest (Pennycook, 1985; Manning et al., 2010). Also, temperature and humidity is important for fungal infection. Pycnidia of *B. dothidea* were formed from 10℃ and disease symptom was developed starting at 9 hours humidity duration (Michailides, 1992; Urbez-Toress et al., 2010). In Jeju, average of temperature was more than 10℃ for conidia formation from March, and average of humidity was more than 60% on every month (Figure 4). In addition, all of Gold3 kiwi cultivar has been cultivated in greenhouse which contributed maintaining high humidity. Therefore, kiwifruits exposure on May to June would be shown high percent of ripe rot infection rate on storage season.

These findings indicate that the Gold3 variety is susceptible to the ripe rot pathogen *B. dothidea*. Therefore, implementing appropriate control measures is crucial to manage ripe rot in the Gold3 variety. Effective chemical control should specifically target the period between May and June for efficient ripe rot management. These studies provide foundational data for controlling ripe rot in Gold3 varieties cultivated in Korea.

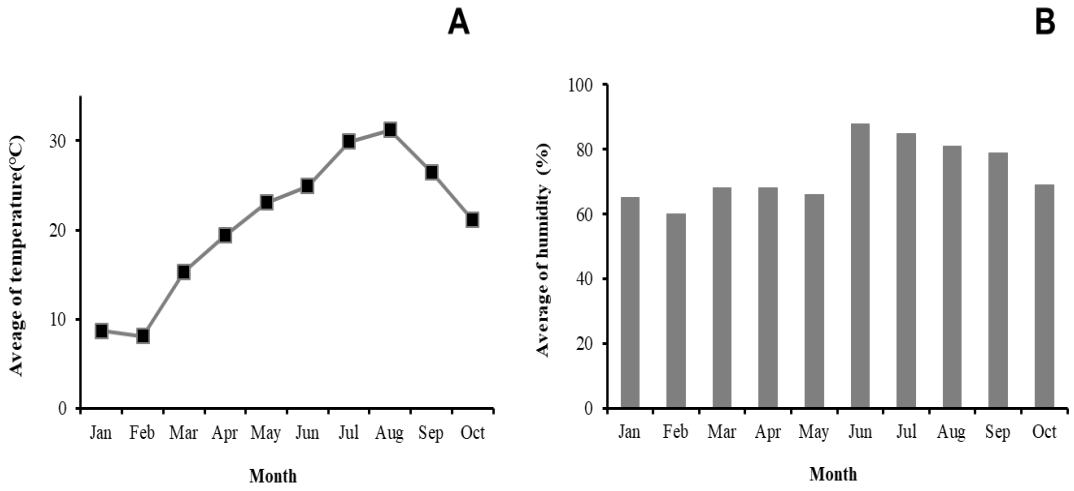

Fig. 4. Jeju Island's climate data sourced from the Korea Meteorological Administration on 2022, illustrating the average temperature (A) and humidity (B) from January to October.

Ⅴ. 적　　요

Botryosphaeria dothidea 에 의해 발병하는 키위 부패병은 제주의 키위농가에 심각한 피해를 주고 있다. 키위 부패병으로부터 키위과실을 효과적으로 보호하기 위해서, 현재 병원균의 빈번도와 병원균감염이 활성화되는 시기를 조사하였다. 키위 부패병의 감염 빈번도를 알기 위하여, 86 개의 키위과실을 10 농가로부터 수거하여 동정하였다. 또한 키위과실을 두 농가에서 11 개의 다른 특정 기간 동안만 노출하여, 수확 후 저장기간 동안 키위 부패병 감염 과실수를 측정하는 병원균 노출 시기 조절 실험 (Window infection)을 수행하였다. 키위 부패병 빈번도 확인검사 결과, 과실 저장성병을 보이는 키위중 76%가 *B. dothidea* 로 동정 되었다. 병원균 노출 시기 조절 실험 결과, 대부분의 키위과실이 착과기인 5 월과 6 월동안 노출하였을 때 키위 부패병이 가장 많이 발생하였다. 본 실험을 토대로, 대부분의 수확 후 병은 *B. dothidea* 로 밝혀졌고, 키위 부패병균을 효과적으로 방제해야 하는 시기는 5 월에서 6 월에 이루어져야 하는 것으로 보인다.

VI. REFERENCES

Aamir, S., Sutar, S., Singh, S. K. and Baghela, A. 2015. A rapid and efficient method of fungal genomic DNA extraction, suitable for PCR based molecular methods. *Plant Pathol. Quar*. 5: 74-81.

Boland, M. 2013. Kiwifruit proteins and enzymes: actinidin and other significant proteins. *Adv Food Nutr Res*, 68:59-80.

Ciacci, C., Russo, I., Bucci, C., Iovino, P., Pellegrini, L., Giangrieco, I., Tamburrini, M. and Ciardiello, M. A. 2014. The kiwi fruit peptide kissper displays anti-inflammatory and anti-oxidant effects in in-vitro and ex-vivo human intestinal models. *Clin Exp Neuroimmunol*, 175(3):476-484.

Deng, H., Li, Y., Pang, C., Zhang, K., Tian, X., Wang, T., Liang, Y., He, Z., Lang, Y., Fang, J., Lin, L., Wang, J., Lv, X., Xia, H. and Liang, D. 2023. Significant increases in Donghong kiwifruit yield by a novel umbrella-shaped trellis system and identification of associated molecular mechanisms. *Front Plant Sci*, 14:1143525.

Donati, I., Buriani, G., Cellini, A., Mauri, S., Costa, G. and Spinelli, F. 2014. New insights on the bacterial canker of kiwifruit (*Pseudomonas syringae* pv. *actinidiae*). *J. Berry Res*. 4:53-67

Ferguson, A. R. 2010. Kiwifruit: evolution of a crop. In VII International Symposium on Kiwifruit 913, pp. 31-42.

Graziani, F., Discepoli, N., Gennai, S., Karapetsa, D., Nisi, M., Bianchi, L., Rosema, N. M. and Van der Velden, U. 2018. The effect of twice daily kiwifruit consumption on periodontal and systemic conditions before and after treatment: A randomized clinical trial. *J Periodontol*, 89(3):285-293.

Jeun, Y. C. 2019. Improving understand of side rot in the orchard (PJ20062). Jeju, South Korea: Jeju National University.

Kim, G. H., Kim, K. H., Son, K. I., Choi, E. D., Lee, Y. S., Jung, J. S. and Koh, Y. J. 2016. Outbreak and spread of bacterial canker of kiwifruit caused by *Pseudomonas syringae* pv. *actinidiae* biovar 3 in Korea. *Plant Pathol J*, 32(6):545.

Kim, G. H., Jung, J. S. and Koh, Y. J. 2017. Occurrence and epidemics of bacterial canker of kiwifruit in Korea. *Plant Pathol J*, 33(4):351.

Kim, G.H. and Koh Y.J. 2018a. Diagnosis and control of major leaf diseases on kiwifruit in Korea. *Res. Plant Dis*, 24(1), 1-8.

Kim, G.H. and Koh Y.J. 2018b. Incidence Rates of Major Diseases on Green-Fleshed Kiwifruit cv. Hayward and Yellow-Fleshed Kiwifruit cv. Haegeum. *Res. Plant Dis*, 24: 175-181.

Kim, G. H. and Koh, Y. J. 2018c. Diagnosis and integrated management of major fungal fruit rots on kiwifruit in Korea. *Res. Plant Dis*, 24(2):113-122.

Kim, S. H., Kang, S. K., Park, S. K. and Kwack, Y. B. 2020. Grafting characteristics of several kiwifruit cultivars as affected by rootstocks. *Agricuiture Research Journal*, 22(1):27-33.

Kim, W. T., Choi, K. L., Lee, H. I., Kim, J. H. and Kim, J. Y. 2023. Chapter 14 fruit supply and demand trends and outlook. Korea Rural Economic Institute Other Research Reports, 533-618.

Ko, S. C., Sung, M. S., Ko, S. H. and Kang, S. G. 2016. Growth specific of kiwifruit of new variety ‘Mega-Green Kiwi (TSECHELIDIS)’ in Jeju. *Hortic. Sci. Technol*, 167-167.

Koh, Y. J. and Lee, D. H. 1992. Kiwi bacteria canker caused by *Pseudomonas syringae* pv. *Morsprunorum*. *Plant Pathol J*, 8(2), 119-122.

Koh, Y. J., Lee, J. G., Lee, D. H. and Hur, J. S. 2003. *Botryosphaeria dothidea*, the causal organism of ripe rot of kiwifruit (*Actinidia deliciosa*) in Korea. *Plant Pathol J*, 19(5): 227-230.

Koh, Y.J., Hur J.S. and Jung J.S. 2005. Postharvest fruit rots of kiwifruit (*Actinidia deliciosa*) in Korea *New Zealand Journal of Crop and Horticultural Science*,33: 303-310.

Koh, Y. J., Kim, G. H., Koh, H. S., Lee, Y. S., Kim, S. C. and Jung, J. S. 2012. Occurrence of a new type of *Pseudomonas syringae* pv. *actinidiae* strain of bacterial canker on kiwifruit in Korea. *Plant Pathol J*, 28(4):423-427.

Koh, Y. J., Kim, G. H. and Jung, J. S. 2017. A proposed manual for the efficient management of kiwifruit bacterial canker in Korea. *Res. Plant Dis*, 23(1):1-18.

Kwack, Y. B., Lee, M. H., Kim, H, L., Chae, W. B., Kim, S. H. and Kang, S. K. 2022. Green-fleshed Sweet Kiwifruit 'Garmrok'. *J. Korean Soc. Int. Agric*, 34(1):43-48.

Kwack, 2022. Overview of kiwifruit industry and research in Korea. *Hortic. Sci. Technol*, 39-40.

Kwon, S. Y., Kim, G. H., Koh, Y. J., Lee, Y. S., Shon, S. H., Kim, S. C. and Jung, J. S. 2011. Incidence rates of postharvest fruit rots and detection rates of their pathogens on new kiwifruit cultivars bred in Korea. *J. Korean Soc. For. Sci.*, 24(5):599-603.

Latocha, P., Krupa, T., Wołosiak, R., Worobiej, E. and Wilczak, J. 2010. Antioxidant activity and chemical difference in fruit of different *Actinidia* sp. *Int J **Food** Sci Nutr*, 61(4), 381-394.

Ledesma, M. 2020. Diagnosis of pathogenic fungus causing dimple rot on Gold3 kiwifruits in Jeju Island, M.S. thesis. Jeju National University, Jeju, Korea.

Ledesma, M., Shin Y. H., Whiteman S, Tyson J. L., Gyoung H. K., Hong, J. K., Zange, B. and Jeun YC 2021. Causal fungus of side rot on 'Zesy002' kiwifruit in Jeju Island, South Korea. *Res. Plant Dis*, 27(1): 24-31.

Lee, Y. S., Kim, G. H., Song, Y. R., Oh, C. S., Koh, Y. J. and Jung, J. S. 2020. Streptomycin resistant isolates of *Pseudomonas syringae* pv. *actinidiae* in Korea. *Res. Plant Dis*, 26(1), 44-47.

Marsberg, A., Kemler, M., Jami, F., Nagel, J. H., Postma-Smidt, A., Naidoo, S., Wingfield, M. J., Crous, P. W., Spatafora, J. W., Hesee, C. N., Robbertse, B. and Slippers, B. 2017.

Botryosphaeria dothidea: a latent pathogen of global importance to woody plant health. *Mol Plant Pathol*, 18(4):477-488.

Manning, M. A., Meier, X., Olsen, T. L. and Johnston, P. R. 2003. Fungi associated with fruit rots of *Actinidia chinensis* 'Hort16A' in New Zealand. *N Z J Crop Hortic Sci*, 31(4):315-324.

Michailides, T. J. and Morgan, D. P. 1992. Effects of temperature and wetness duration on infection of pistachio by Botryosphaeria dothidea and management of disease by reducing duration of irrigation. *Phytopathology*, 82(12):1399-1406.

Nazerian, E., Mirabolfathy, N., Ashnaei, S. P. and Beiki, F. 2019. Characterization of *Botryosphaeria dothidea* as new pathogen of kiwifruit in Iran. *J Plant Prot Re* ,59(1).

Pennycook, S. R. 1985. Fungal fruit rots of *Actinidia deliciosa* (kiwifruit). *N Z J Crop Hortic Sci*, 13(4):289-299.

Ren, Y., Wang, T., Tang, J., Jiang, Y., Huang, Y., Zhang, C., Peng, J., Wang, J., Wang, S. and Wang, J. 2022. Identification of the pathogens and laboratory bioactivity determination of the rot disease of kiwifruit (*Actinidia* spp.). *J Chem*, 2022:2293297.

Richardson, D. P., Ansell, J. and Drummond, L. N. 2018. The nutritional and health

attributes of kiwifruit: A review. *Eur J Nutr*, 57:2659-2676.

Saitou, N. and Nei, M. 1987. The neighbor-joining method: a new method for reconstructing phylogenetic trees. *Mol Biol Evol*, 4(4):406-425.

Singletary, K. 2012. Kiwifruit: overview of potential health benefits. *Nutr Today*, 47(3):133-147.

Suksomboon, N., Poolsup, N. and Lin, W. 2019. Effect of kiwifruit on metabolic health in patients with cardiovascular risk factors: A systematic review and meta-analysis. *Diabetes Metab. Syndr. Obes*, 171-180.

Tyagi, S., Nanher, A. H., Sahay, S., Kumar, V., Bhamini, K., Nishad, S. K. and Ahmad, M. 2015. Kiwifruit: Health benefits and medicinal importance. *Rashtriya krishi*, 10(2):98-100.

Urbez-Torres, J. R., Bruez, E., Hurtado, J. and Gubler, W. D. 2010. Effect of temperature on conidial germination of *Botryosphaeriaceae* species infecting grapevines. *Plant dis*, *94*(12):1476-1484.

Wang, S., Qiu, Y., and Zhu, F. 2021a. Kiwifruit (*Actinidia* spp.): A review of chemical diversity and biological activities. *Food Chem*, 350:128469.

Wang, L., Hou, H., Zhou, Z., Tu, H. and Yuan, H. 2021b. Identification and detection of *Botryosphaeria dothidea* from kiwifruit (*Actinidia chinensis*) in China. *Plants (Basel)*, 10(2):401.

Yang, H. Y., Wang, W. H., Zhan, J. Y., Huang, Y. L. and Cheng, W. Y. 2020. Beneficial Effects of Golden Kiwifruit Consumption in Overweight and Obese Young Adults. *J. Nutr. Sci. Vitaminol*, *66*(Supplement): S356-S360.

Zhang, C., Long, Y. H., Wang, Q. P., Li, J. H., Wu, X. M. and Li, M. 2019. The effect of preharvest 28.6% chitosan composite film sprays for controlling the soft rot on kiwifruit. *Zahradnictvi (Praha)*, 46(4):180-194.

Zhou, Y., Gong, G., Cui, Y., Zhang, D., Chang, X., Hu, R., Liu, N. and Sun, X. 2015. Identification of Botryosphaeriaceae species causing kiwifruit rot in Sichuan Province, China. *Plant Dis*, 99(5):699-708.

Part B. Genetic control in kiwifruit against ripe rot

List of Figures

List of Tables

ABSTRACT

The ascomycete fungus *Botryosphaeria dothidea* is the causal agent of postharvest rot in kiwifruit. Production and spreading of conidia, differentiation of infection hyphae and invasion of intact fruit surfaces are required to cause fruit rot disease. In several pathogenic fungi, the homolog of the *Saccharomyces cerevisiae* mitogen activated protein kinase (MAPK) gene *Fus3* has been identified as a pathogenicity factor. To investigate the role of the *Fus3* homolog in *B. dothidea*, the gene was deleted and the resulting Δ*fus3* mutants were characterized. On artificial media, strong growth defects of Δ*fus3* strains were observed and mycelia were non-pigmented, and mutants were unable to conidiate. Scanning electron microscopy showed that the wildtype strain differentiated thick hyphae on the surface of kiwifruits, and nose-down growth of hyphae indicated tight attachment to the fruit. By contrast, hyphae of Δ*fus3* strains mutants were thinner and did not firmly attach to the fruit surface. Importantly, pathogenicity test revealed that Δ*fus3* strains were unable to cause disease symptoms on intact kiwifruits. These results shown here identify *Fus3* of *B. dothidea* as a novel pathogenicity factor of the ripe rot pathogen on kiwifruit.

Key words: gene deletion, infection process, melanin, mutant, ripe rot, ultrastructure

I. INTRODUCTION

Botryosphaeria dothidea is an ascomycete with a wide host range. It attacks woody plants such as pistachio, acacia, eucalyptus, grape, and apple (Michailides et al., 1998; Marsberg et al., 2017; Wang et al., 2021). Ripe rot control is carried out using synthetic chemical fungicides such as benomyl, thiophanate-methyl, tebuconazole, iprodione, and flusilazole has been currently used for field application (Koh et al., 2005). However, the use of the synthetic fungicides has been controversially discussed with respect to human health and environmental risks (Deising et al., 2017; Oliveira-Garcia et al., 2021), leading to increased employment of putatively eco-friendly materials instead of the synthetic chemicals (Dai et al., 2022; Di Francesco et al., 2016;). Recently, some of eco-friendly materials were reported to control the ripe rot caused by *B. dothidea*. Indeed, the symptom severity of ripe rot on kiwifruit was reduced after application of chitosan (Zhang et al., 2020), methyl jasmonate (Pan et al., 2020), or crude extract of eucalyptus (Oh et al., 2008). In addition, the development of ripe rot symptoms was inhibited when rhizobacterial strains such as *Bacillus subtilis* or *B. amyloliquefaciens* were applied (Kim and Ko, 2015; Pang et al., 2021; Fan et al., 2023).

Besides, genetic engineering of crops is among the most promising strategies in plant protection. Schweizer and co-workers have employed essential genes of the barley powdery mildew fungus *Blumeria graminis* f. sp. *hordei* to establish a method called *host-induced gene silencing* (HIGS) (Nowara et al., 2010). RNA interference (RNAi) constructs of essential mildew genes were expressed in barley plants, and interfering RNAs targeting the fungal genes were taken up by the infecting fungus, leading to reduction of the transcript

abundance of the target gene, and reduced disease incidence. Also, against non-biotrophic pathogens, i.e. different *Fusarium* species infecting cereals, HIGS has been shown to be effective (Chen et al., 2016). More recent developments known as spray-induced gene silencing (SIGS) have shown that gene silencing in a pathogen may also occur after spraying RNAi constructs directed against important fungal genes RNAi constructs can be employed by spray-application (Koch et al., 2016; Koch et al., 2017). This method employs double-stranded RNAs (dsRNAs) homologous to essential transcripts of a pathogen, either transcripts indispensable for general metabolism of for pathogenic development. In brief, dsRNAs are sprayed onto the surface of a plant to be protected, and after uptake of the dsRNA the RNA-induced silencing complex identifies and degrades the essential target RNA. Hence, any gene required for vegetative and/or pathogenic development could serve as a candidate gene for SIGS (Koch et al., 2016; Sarkar and Barman 2021; Qiao et al., 2021; McRae et al., 2023). Based on the broad range of pathogens that could putatively be controlled by HIGS or SIGS, the identification of essential genes in economically relevant pathogens is strongly advised.

Fungal mitogen activated protein kinases (MAPK) have been shown to be important factors governing the outcome of host infection (Hamel et al., 2012). Though first characterized in *S. cerevisiae*, the genomes of all pathogens investigated so far harbor several MAPK genes, several of which have been shown to be required for pathogenicity (Lin et al., 2010; Tsai et al., 2013; Xiong et al., 2015). In *S. cerevisiae*, three MAPK cascades; Fus3, Slt2, and Hog1, in *Saccharomyces cerevisiae* (Turra et al., 2014), Fus3 has a role for expression the mating hormone related to promote cell growth and cell to cell recognition (Chen and Thorner, 2007; Sumita et al., 2019; Madhani and Fink, 1998). Slt2 is pivotal for maintaining the cell wall integrity (Martin et al., 2000), Hog1 has a role in osmotic, cold and heat stress signaling (Mizuno et al., 2015; Baranwal et al., 2014). Intriguingly, in plant pathogenic fungi Fus3 appears to control formation of infection cells called appressoria, and

has therefore a direct impact on pathogenic development (Xu and Hamer, 1996; Takano et al., 2000).

In spite of the enormous postharvest losses caused by *B. dothidea* on kiwifruit alone, the fungus has been poorly studied on the molecular level and, hence, candidate genes that could be addressed as targets in SIGS are unknown. In this study, we established targeted gene deletion to characterize the MAPK gene *FUS3*. Δ*fus3* mutant strains showed vegetative growth and pigmentation defects, and were defective in asexual sporulation. Hyphae formed by Δ*fus3* strains were significantly thinner than those of the WT strain and exhibited adhesion defects. Importantly, on kiwifruits Δ*fus3* strains were unable to cause ripe rot disease. We show here for the first time that the MAPK gene *FUS3* of *B. dothidea* is indispensable for pathogenicity.

II. MATERIALS AND METHODS

1. Isolation of *B. dothidea* from ripe rot lesions of kiwifruits

A wildtype (WT) strain of the fungus *Botryosphaeria dothidea*, causing ripe rot on kiwifruits, was isolated from an infected fruit of *Actinidia chinensis* cultivar 'Gold3' as described (Ledesma et al. 2021).

For pathogen identification, DNA was extracted from the mycelium (Aamir et al., 2015), and the internal transcribed spacer (ITS) region was amplified using primers ITS1 and ITS4 (Supplemental Table 1). DNA fragment at 581bp was sequenced (Macrogen, Seoul, Korea) and sequence comparisons using the NCBI blast service identified the fungus as *B. dothidea*.

2. Identification of the *B. dothidea FUS3* gene and generation of a deletion cassette

The Fus3 amino acid sequence of *Saccharomyces cerevisiae* was used as query to identify the Fus3 protein of *B. dothidea* by Blastp (https://blast.ncbi.nlm.nih.gov/). To compare the relatedness of the Fus3 protein of *B. dothidea* with the orthologue of *S. cerevisiae* and seven filamentous ascomycete plant pathogens, a phylogenetic tree was generated using NCBI using maximum likelihood analyses with the MEGA software program (Ver. 11.0.13)(Taylor and Berbee, 2006).

The MAPK gene *FUS3* of *B. dothidea* with the accession Number KAF4301461.1 was used to generate the deletion construct part in genome sequence data of *B. dothidea* (accession number: GCA_011503125.2). For double joint PCR, the 5'- and the 3'-flank was PCR-amplified, using genomic DNA of *B. dothidea* and primer pairs NBDOLF-F and NBDOLF-R, and NBDORF-F and NBDORF-R, yielding ca. 1,000 bp each of the 5'-flank and 3'-flang of *FUS3*, respectively. The plasmid pJET1.2 containing the nourseothricin resistance gene (*nat 1*) and primers Nourseo-F and Nourseo-R (Malonek et al., 2004) were used to amplify the nourseothricin resistance cassette. The nourseothricin resistance cassette and the 5'- and 3'-flank were fused by Double-Joint-PCR, using nested primers NBDONes-F and NBDONes-R (Yu et al., 2004). For PCR reactions Taq polymerase (iNtRON Bio, Sungnam, Korea) or phusion polymerase (ThermoFisher, Waltham, MA, USA) were used. The deletion cassette was purified using a gel purification kit (Genesgene, Busan, Korea) and used for protoplast transformation.

3. Protoplast transformation

Three agar blocks (5 x 5 mm) overgrown by hyphae of *B. dothidea* were inoculated into 200 ml yeast extract sucrose (YES) broth and incubated at 28℃ in a shaking incubator (Hanbaek Scientific Co., Seoul, Korea) at 100 rpm for 5 days. The mycelium was filtered (Advantec®, Toyo Roshi Kaisha, Japan) and washed 3 times with 100 ml of sterilized distilled water. The mycelium was incubated in 10 ml of protoplasting solution, containing 40 mg/ml of lysing enzyme from *Trichoderma harzianum* (Sigma-Aldrich, Seoul, Korea) and 0.1% (v/v) β-mercaptoethanol in 0.7 M sodium chloride at 30℃. The cell wall digestion mix was shaken for 3 h at 80 rpm. Protoplasts were filtered with double layers of Miracloth (Calbiochem, La Jolla, CA) and centrifuged at 14,000 x *g* at 4℃ for 10 min, and the pellet was washed with 10 ml SCT (1 M sorbitol, 50 mM $CaCl_2$, and 50 mM Tris-HCl, pH 8.0). After centrifugation, the pellet was re-suspended in SCT, adjusted to contain $2x10^7$ protoplasts / ml, mixed with 5 μg of the deletion cassette and incubated on ice for 30 min. One ml of polyethylene glycol (PEG) solution (40% [w/v] PEG 4000; 0.6 M KCl, 50 mM $CaCl_2$, and 50mM Tris-HCl, pH 8.0) was added and incubated for 20 min at room temperature. The protoplast suspension was diluted with 10 ml liquid regeneration medium (1 M sucrose; 0.1% (w/v) yeast extract, 0.1 % (w/v) casein, and 0.6 % (w/v) agar), poured onto selection medium (regeneration medium amended with 0.4 mg nourseothricin / ml and solidified by 1.5% agar) and incubated at 28℃ for 5 days. Colonies growing on selection medium were further grown on YES containing 0.4 mg nourseothricin / ml. DNA was extracted as described above and tested by PCR using primers NBDOCheck-F and NBDOCheck-R (Supplemental Table S1).

4. Southern blot analyses

Southern blot based on Roche's DIG application manual (Roche Applied Science) were carried out with the candidates of mutants of which target gene were deleted. Total 10μg of DNA was digested with *EcoRV* enzyme (Thermo Scientific, Waltham, USA) for at 37℃ for 16 h. Digestion completed DNA was loaded with 0.8 % (w/v) Tris-Acetate EDTA (TAE) gels electrophoresis at 60mV for 2 h and denature solution (0.5M sodium hydroxide and 1.5M sodium chloride) and neutralized solution (0.5M tris hydrochloride and 1.5M sodium chloride pH 7.5) were treated for 30 m with smooth shaking, respectively. After electrophoresis separated DNA fragment was transferred to positively charged nylon membranes (Sigma-Aldrich, Madrid, Spain) by capillary transfer methods (Chomczynski, 1992) using 20X SSC buffer (3M sodium chloride, 0.3M sodium citrate dehydrate pH 7.0) at room temperature for overnight. Transferred membrane was dried at 80℃ for 2 h and incubated with 10ml of Perfect Hyb-Plus buffer (Sigma Inc, USA) in a hybridization oven (UVP hybridizer oven, Analytik Jena, Jena, Germany) at 68℃ for 20min. Fresh Perfect Hyb-Plus buffer adding with 500ng of Dig-labelled probe amplified using DNA dig labeling mix (Roche, Mannheim, Germany) was added and incubated at 68℃ for overnight. Probe of 572bp was amplified from genomic DNA of *B. dothidea* with BDPro-F (5′-CCAAACGCCCTCCACTAATG-3′) and BDPro-R (5′-CAAAGCCCAGCAGCTAATCC-3′) primers targeting to right flank part of the cassettes. The membrane was washed with 2X washing solution (2X SSC, 0.1% SDS) at 68 ℃ for 5 mins two times and each 0.5X and 0.25X washing solution carried out at 68℃ for 15 mins. The membrane was washed with washing buffer M (0.1M malic acid, 0.15M sodium chloride, and 0.3% tween pH 7.5) at

room temperature for 1 min. Washed membrane was incubated in blocking solution (0.2M tris base, 1.37M sodium chloride, pH7.6) containing 0.2% I-Block reagent (Tropix, Bedford, MA, USA) in 10X tris-buffered saline and 2µl of AP-conjugated anti-DIG antibody (Roche) was added to fresh blocking solution. The membrane was washed with washing buffer M for 10 mins for three times and incubated in detection buffer at pH 9.5 (0.1M tris hydrochloride, 0.1M sodium chloride) for 2 mins. The membrane was inserted to hybridization bag and 1ml of CSPD (CSPD ready-to-use, Roche, Mannheim, Germany) with 1ml detection buffer (0.1M tris hydrochloride, 0.1M sodium chloride pH 9.5) was added to membrane and the bubbles were removed to edge of hybridization bag and sealed. The blot images were visualized using documentation system (Chemidoc, Bio-Rad, Milan, Italy).

5. Vegetative development

To compare growth of the *B. dothidea* WT and Δ*fus3* strains, PDA plates were inoculated with an agar block (ø = 7 mm) and incubated at 28℃. Similarly, three agar blocks were inoculated into potato dextrose broth (PDB; Becton, Dickinson and Company, Claix, France) and incubated in a shaking incubator (HB-201SL, Hanbaek Scientific Co., Bucheon, Korea) at 80 rpm and 28℃ for 2 days. To quantify vegetative development, the diameter of mycelium and the fungal fresh and dry mass were measured. Conidia formed on oatmeal agar were washed with 10 ml sterilized water using loop and concentrations were measured using a hemocytometer (Hausser Scientific, Horsham, PA, USA).

6. Pathogenicity test

Fruits of *Actinidia chinensis* cv. 'Gold3' were imported from New Zealand and obtained from the commercial market. To compare virulence of *B. dothidea* WT and Δ*fus3* strains on kiwifruits, three agar blocks colonized by mycelium of *B. dothidea* were placed upside down onto unwounded kiwifruits and incubated in an incubator (DA MIL-2500, Dong-A, Siheung, Korea) at 90% relative humidity and 28℃ for 10 days. Diameters of rot symptoms formed at infection sites were used as a measure of virulence.

7. Microscopy

Vegetative hyphae of WT and Δ*fus3* strains grown in PDA were observed by bright field microscopy (Leica DM750 Microsystems, Wetzlar, Germany) at 10 dip.

For scanning electron microscopy, blocks of the inoculation sites (5 x 5 mm^2) of *A. chinensis* cv. 'Gold3' were excised and pre-fixed with 2% (v/v) glutaraldehyde in 0.05M sodium hydrogen phosphate (pH 7.2) for 2 h at 4℃. The samples were washed three times with phosphate buffer (0.05M NaH_2PO_4 / Na_2HPO_4, pH 7.2) for 10 min and post-fixed with 1%

(w/v) osmium tetroxide in phosphate buffer (0.05M NaH_2PO_4/ Na_2HPO_4, pH 7.2) at 4℃ for 2h. The tissues were washed twice with sterilized distilled water for 10 min and dehydrated with an ethanol series of 30, 50, 70, 80, and 90% (v/v) for 10 min. each, and incubated three times in 100% ethanol (v/v) for 30 min. Dehydrated samples were dried with a critical point dryer (Leica EM CPD 300 Critical Point Dryer, Leica Microsystems, Wetzlar, Germany) for 2 h and coated using a sputter coater (Q150TS, Quorum Technologies, UK) with platinum at 20 mv for 2 minutes. The coated samples were observed with a field emission scanning electron microscope (FESEM MIRA3, Tescan, USA) at 5 kV.

8. Statistical analysis.

The data length of mycelia on PDA, weight of mycelia on PDB, conidia concentration on OMA, diameter of lesion size on kiwifruit, and diameter of hyphae thickness for compare fungal characteristics between wildtype and mutants were analyzed with Duncan's multiple range test, using SAS version 9.0 (SAS Institute Inc., Cary, NC, USA). Statistical significance was considered at $P < 0.05$.

III. RESULTS

1. Fungal strain identification and gene characteristic

ITS sequencing and Blastp comparisons showed 99% nucleotide identity with the published ITS sequence of the *B. dothidea* type strain UCD2467TX (accession number: FJ790847.1). In order to confirm the authenticity of Fus3 of *B. dothidea*, Blastp comparisons with Fus3 homologs of the ascomycete yeast *S. cerevisiae* and with the plant pathogenic filamentous ascomycetes *Alternaria alternata*, *Alternaria brassicicola*, *Fusarium graminearum*, *Colletotrichum lagenarium*, *Pyricularia oryzae*, *Verticilluim dahliae*, and the basidiomycete wheat stripe rust fungus *Puccinia striiformis* were made. The phylogenetic tree shows that Fus3 of *B. dothidea* is most closely related to the *Alternaria* Fus3 proteins. The amino acid sequence of the *B. dothidea* Fus3 protein showed 60% identity with the yeast homolog and was designated as Fus3 (accession number: KAF4301461.1). In result, *B. dothidea* Fus3 is closely related to the yeast *S. cerevisiae* as other filamentous pathogenic ascomycetes such as *Fusarium graminearum* (AAL73403.1), *Colletotrichum lagenarium* (accession number: AAD50496.1), *Pyricularia oryzae* (accession number: Q92246.2), *Verticilluim dahlia* (accession number: AAW71477.1), *Alternaria brassicicola* (accession number: AAS20192.1) or *Alternatia altanata* (accession number: ACY73851.1) (Supplemental Fig. 2).

2. Targeted deletion of *Fus3*

To delete the 3,972 bp *FUS3* gene of *B. dothidea* by homologous integration, a deletion cassette consisting of 1,033 bp of the left and 1,029 of right flanks of *FUS3*, respectively, and the 1,433 bp nourseothricin resistance cassette was generated (Fig. 1A; Supplemental Fig. S2). The final 3,379 bp deletion cassette was amplified by double joint PCR (Supplemental Fig. 3) and transformed into protoplasts of *B. dothidea*. Of 38 randomly selected nourseothricin-resistant colonies DNA was extracted, and a PCR screen with primers NBDOCheck-F and NBDOCheck-R yielded 8 transformants lacking a *FUS3* fragment (Supplemental Fig. 4 and Supplemental Table 2.). DNA extracted from these transformants was digested with *EcoRV* and subjected to Genomic Southern Blot analyses (Fig. 1B). As expected, the WT strain showed a 3.4 kb band indicative of the *FUS3* gene, whereas all three independent Δ*fus3* strains used in this study showed a 1.8 kb band (Fig. 1A and B).

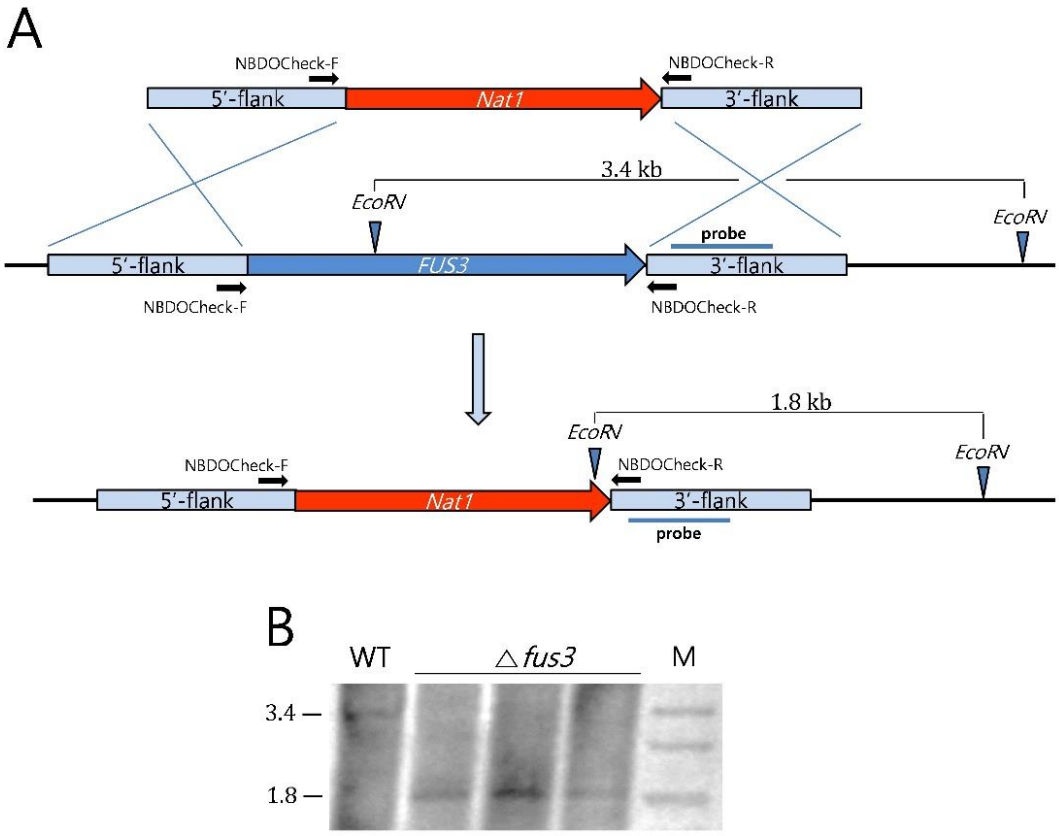

Fig. 1. Targeted deletion of the MAP kinase gene *FUS3* of *B. dothidea*. **A**. Homologous integration of the deletion construct leads to replacement of the *FUS3* gene by the nourseothricin resistance gene *Nat1*, resulting in an *Eco*RV fragment size polymorphism. **B**. Southern blot showing a 3.4 kb and 1.8 kb *Eco*RV fragments in the WT and Δ*fus3* mutants, respectively. Localization of the Digoxygenin-labelled probe used for hybridization is indicated in **A**. M, DIG-labeled DNA molecular weight marker Vll (Sigma-Aldrich, Co.Ltd).

3. Vegetative development of *B. dothidea* WT and Δ*fus3* strains

To compare the growth rates and colony phenotypes of the *B. dothidea* WT and Δ*fus3* strains, agar blocks of *B. dothidea* mycelia were inoculated onto PDA. Colony diameters of the Δ*fus3* mutants were smaller than those of the WT strain over 3 days (Fig. 2A, B). On OMA the WT and Δ*fus3* strains had covered the entire plate at 10 dpi, and the WT strain, but not the Δ*fus3* strains had started strong pigment formation (Fig. 2; 10 dpi). Interestingly, on PDA the WT strain formed a loose mycelium with large numbers of aerial hyphae (Fig. 2 C, WT, arrow), and hyphae grew out onto the substratum forming a soft mycelial margin (Fig. 2 C, WT, arrowhead). By contrast, the mycelium of Δ*fus3* strains appeared dense (Fig. 2 C, Δ*fus3*, arrow) and exhibited a rigid edge at the interface with the substratum (Fig. 2 C, Δ*fus3*, arrowhead). In liquid PD broth (PDB) WT and Δ*fus3* strains formed round ball-like colonies (Fig. 3A), and both fresh and dry weight measurement revealed that Δ*fus3* strains had formed less fungal mass than the WT strain at 2 dpi (Figures 3B and C).

Moreover, scanning electron microscopy of mycelia grown on OMA revealed that many of conidia were produced by the WT strain (Fig. 4A, WT, arrowheads; Fig. 4B), with few vegetative hyphae visible only (Fig. 4A, WT, arrow). In comparison, Δ*fus3* strains only formed vegetative hyphae in great abundance, but conidia were not detected (Fig. 4A, Δ*fus3*, arrows; Fig. 4B).

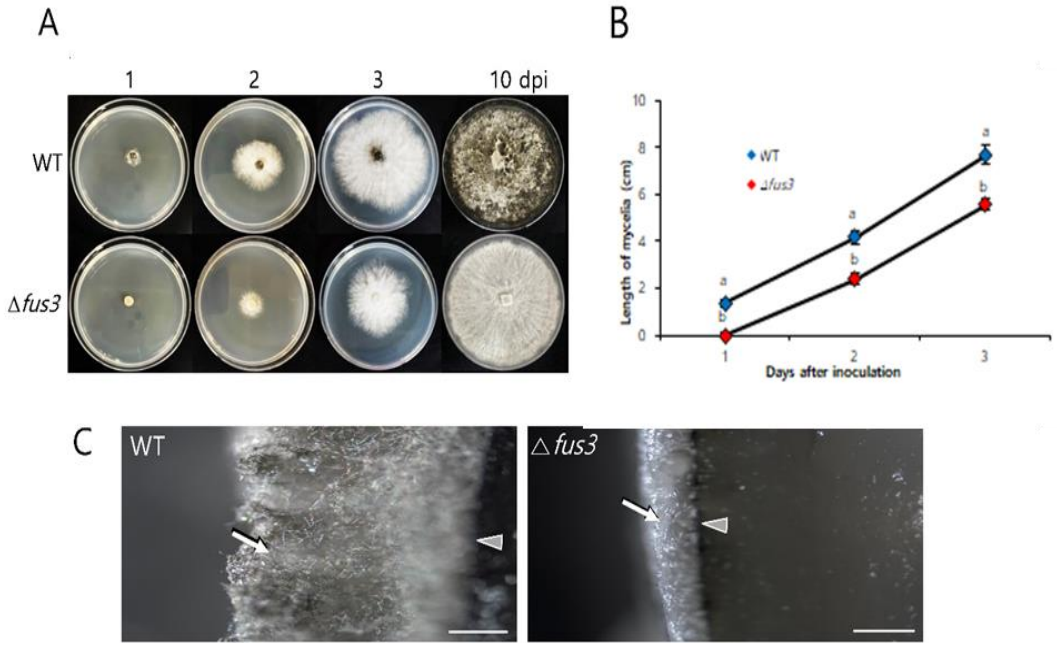

Fig. 2. Colony phenotype of WT and Δ*fus3* mutants of *B. dothidea*. **A**. Colony phenotypes of WT and Δ*fus3* mutants on PDA at 1, 2, and 3 dpi, and on OMA at 10 dpi. Note strong pigmentation of the WT and lack of pigmentation of the Δ*fus3* strain on OMA at 10 dpi. **B**. Colony diameter of the WT and Δ*fus3* strains at 1, 2, and 3 dpi. Bars are standard deviations, different letters denote statistical distinctness at $P < 0.05$. **C**. Margins of WT and Δ*fus3* colonies. While the WT strain forms a fluffy mycelium with aerial hyphae (WT, arrow), Δ*fus3* strains form compact mycelia lacking aerial hyphae (Δ*fus3*, arrow). Margins of the WT strain appear soft, those of the Δ*fus3* strain are discrete.

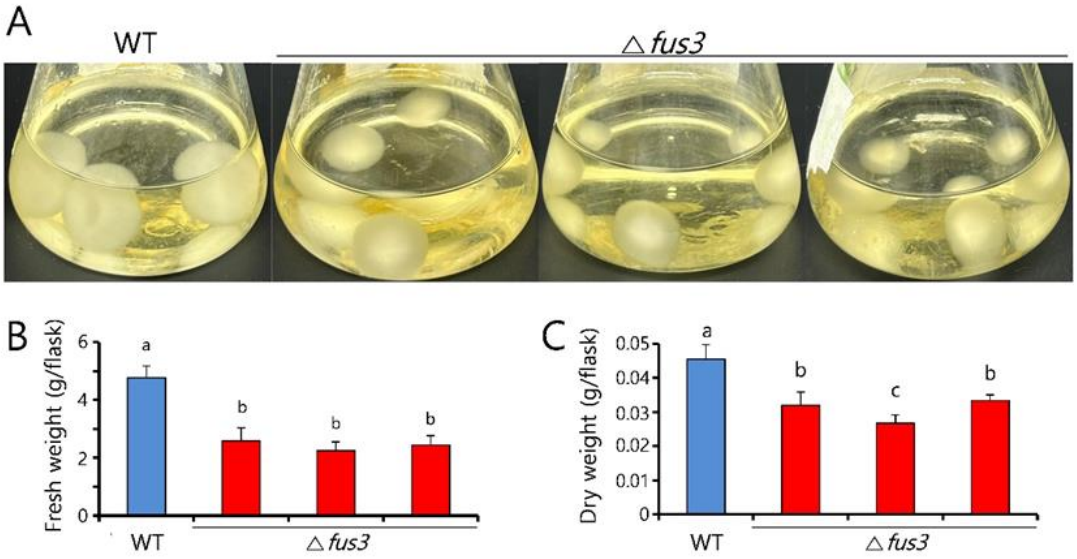

Fig. 3. Development of WT and Δ*fus3* strains of *B. dothidea* in PDB. A. Ball-like colonies of the Δ*fus3* mutants remain smaller than those of the WT strain. Photos were taken at 2 dpi. B. and C. indicate fresh and dry weight of WT and Δ*fus3* strains. Bars are standard deviations, different letters indicate statistical distinctness at $P < 0.05$.

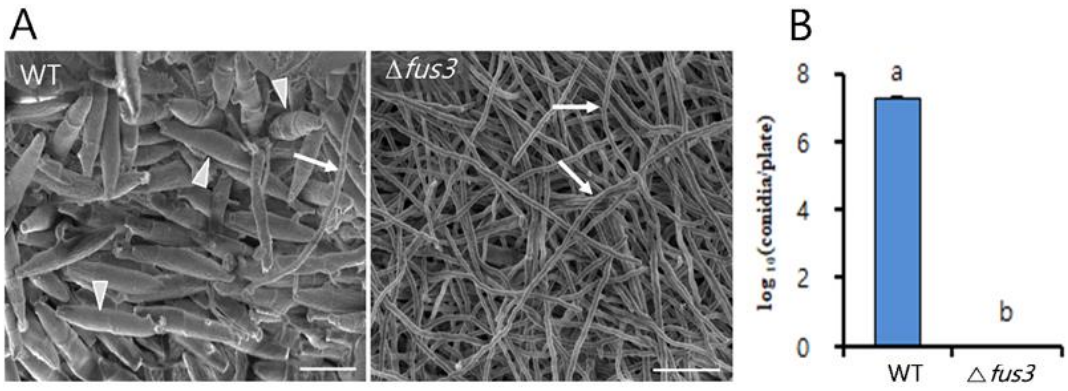

Fig. 4. Asexual sporulation of the WT and Δ*fus3* strains of *B. dothidea*. A. SEM shows that the WT strain forms numerous conidia on PDA (WT, arrowheads), leaving only few hyphae (WT, arrow) uncovered. In contrast, Δ*fus3* strains fail to produce conidia, with many vegetative hyphae visible on PDA plates (Δ*fus3*, arrows). Size bars are 10 µm. B. Plates were washed with 10 ml, conidia were counted using a hemocytometer, and concentrations are given as $\log_{10}$-transformed values. Bars indicate standard deviations. Different letters indicate statistical distinctness at $P < 0.05$.

4. Pathogenicity of the Δ*fus3* mutants

To study the role of Fus*3* of *B. dothidea* in the pathogenicity, we inoculated agar plugs covered with *B. dothidea* hyphae onto intact kiwifruits. Kiwifruits inoculated with the WT strain had formed dark lesions on the fruit surface (Fig. 5A, top row, WT, arrowhead), and through the intact skin of the fruit soft rotting became visible (Fig. 5A, top row, WT, area indicated by arrows). Indeed, after excision of the skin, soft rotted fruit tissue caused by the WT strain was readily visible (Fig. 5A, WT, lower row, black arrow). By contrast, the Δ*fus3* strains remained restricted to the inoculation sites and were non-pigmented at the end of the experiment, i.e. at 10 dpi (Fig. 5A, Δ*fus3*, top row, arrowhead). Intriguingly, after removal of the skin of the fruit, no rotting symptoms were observed (Fig. 5A, lower row, white arrows). Quantification of lesion diameters clearly highlighted the difference in virulence between WT and Δ*fus3* strains on kiwifruits (Fig. 5B).

As Δ*fus3* mutants were unable to produce spores, this mode of inoculation had to be used to keep the inoculation procedure with WT and mutants comparable. From the agar blocks hyphae colonized the fruit surface and attempted invading the fruit tissue. Intriguingly, scanning electron microscopy revealed that *FUS3* greatly affects hyphal pre-penetration development on the fruit surface. At 10 dpi, the WT strain had formed voluminous epicuticular hyphae on the kiwifruit surface (Fig. 6A, WT, arrows, Fig. 6B) from which short hyphae grew out in a ‘nose down’ fashion (Fig. 6A, WT, arrowhead), indicative of an adhesive and host-invading structure. For comparison, host surface-localized hyphae of Δ*fus3* mutants were thin (Fig. 6A, Δ*fus3*, arrows, Fig. 6B). Short hyphae developed from these thin hyphae, but appeared not to be intact and not firmly attached to the surface of the kiwifruit (Fig. 6A, Δ*fus3*, arrowhead). These differences in pre-penetration development

were expected to cause clear differences in the infection process and ripe rot symptom development.

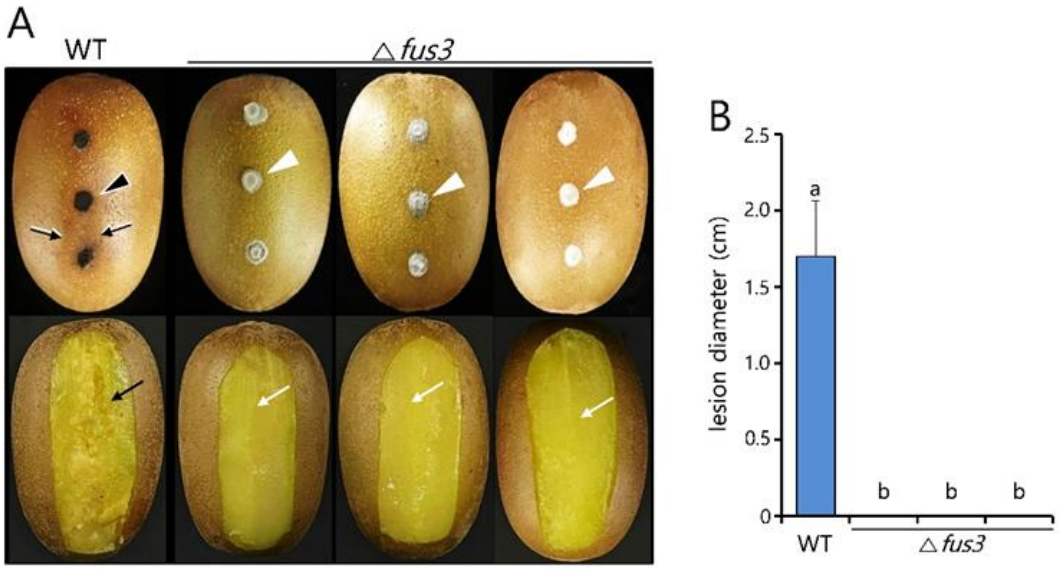

Fig. 5. Virulence assays of WT and Δ*fus3* strains on non-wounded kiwifruits. **A**. Top row: Kiwifruits were inoculated with mycelial plugs and incubated for 10 days. Note that the WT strain formed strongly pigmented mycelia (WT, black arrowhead), which invaded the fruit tissue. The tissue between the black arrows appears softened. By contrast, the mycelial plugs of Δ*fus3* strains remained non-pigmented (Δ*fus3* strains, white arrowhead), and softened tissue could not be seen. Lower row: After peeling the outer skin, macerated tissue is visible in WT-inoculated fruits (black arrow), indicative of fungal colonization. The fruit tissue inoculated with Δ*fus3* strains remained intact (white arrows). **B**. Lesion diameter caused by WT and Δ*fus3* strains. Bar indicates standard error. Different letters indicate statistical distinctness at $P < 0.05$.

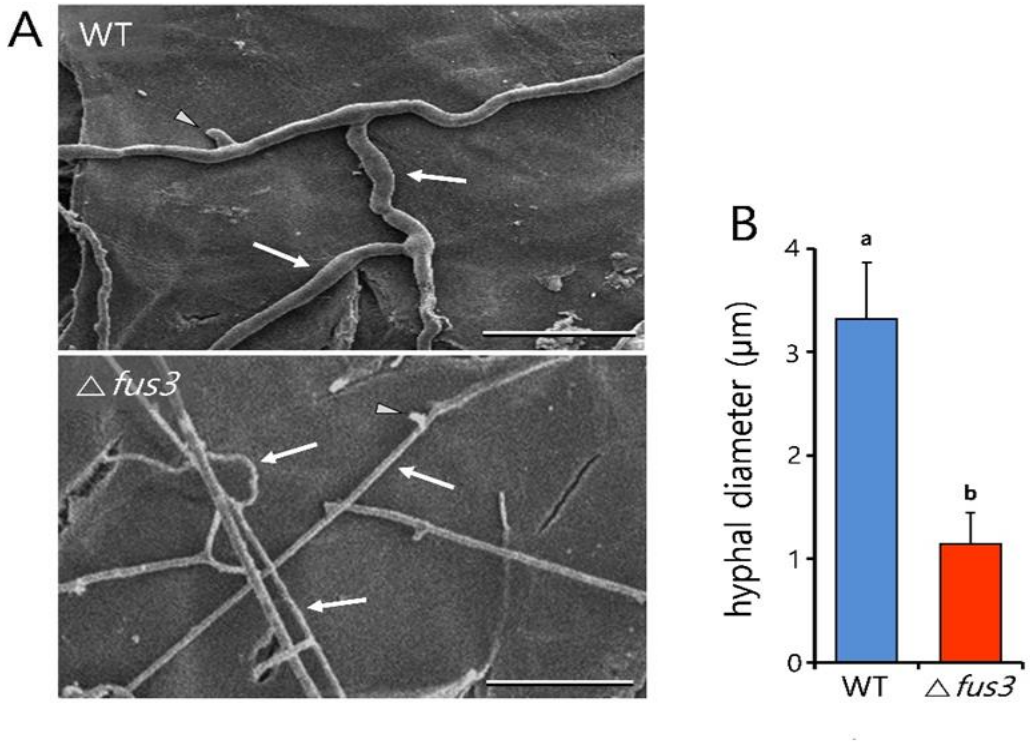

Fig. 6. Hyphae formed on the surface of kiwifruit. **A**. SEM micrograph of WT and Δ*fus3* strains. Arrows indicate surface-localized hyphae; arrowheads point at hyphopodia. Note that hyphae of the Δ*fus3* strain are much thinner than those of the WT. Size bars are 20 μm. **B**. Hyphal diameters of WT and Δ*fus3* strains. Bars give standard deviations, different letters indicate statistical distinctness at $P < 0.05$.

IV. DISCUSSION

Mitogen activated protein kinases (MAPKs) play major roles in vegetative and pathogenic development in microorganisms (Widmann et al., 1999), as demonstrated by targeted gene deletions in several instances (Rodriguez-Iglesias and Schmoll, 2015). As classical fungicides are progressively banned in agriculture (Oliveira-Garcia et al., 2021), alternative technologies are strongly promoted. One of these is spray-induced gene silencing (Koch et al., 2016), which targets fungal genes that are indispensable for pathogenicity. Hence, identifying essential genes in economically important pathogens such as *B. dothidea* may lead to control of kiwifruit ripe rot. Plausibly, targeted gene deletion approaches of candidate genes may indicate their usefulness in agriculture. In this context it is relevant that in several plant pathogenic fungi, homologs of the MAPK gene *FUS3* have been shown to play a role in pathogenesis-related morphogenesis and thus in virulence or pathogenicity.

As part of morphogenesis, mycelia of *B. dothidea* of which target gene mitogen active protein kinase *Fus3* ortholog deleted was grown less at 20-30% on artificial media compared to that of wildtype strain (Fig. 2). Similarly, mycelial growth of *Valsa mali* causing apple valsa canker was reduced on PDA media when *VmPmk1*, *Fus3* related MAPK gene, was deleted (Wu et al., 2017). Also, mycelial growth was decreased not only in *Colletotrichum truncatum* of which *Fus3* related MAPK gene, *CtPMK1*, was knocked out (Xiong et al., 2013) but also in *Aspergillus flavus* Δ*fus3* (Ma et al., 2022).

For example of pathogenicity, deletion strains of *Magnaporthe oryzae* lacking the *FUS3* homolog *PMK1* were not affected in vegetative development and sexual and asexual reproduction, but were unable to differentiate appressoria and failed to invade rice plants and to cause blast disease (Xu and Hamer, 1996). The *PMK1* homolog of *C. lagenarium*, Cmk1,

was able to complement appressorium formation in *M. oryzae* Δ*pmk1* mutants. As in these mutants, Δ*cmk1* mutants failed to form appressoria, to grow invasively in cucumber and to cause anthracnose disease (Takano et al., 2000). In another *Colletotrichum* species, i.e. *C. gloeosporioides*, the Pmk1 homolog *CgMK1* is required for aerial hyphal growth and biomass accumulation (He et al., 2017), and Δ*Cgmk1* mutants thus resemble Δ*fus3* mutants of *B. dothidea* in this respect. Interestingly, *CgMK1* controls the expression of melanin biosynthesis genes and the ability to differentiate appressoria (He et al., 2017), which is in agreement with pigmentation defects of Δ*fus3* mutants of *B. dothidea*. *B. dothidea* does not differentiate appressoria in order to invade its host, but secretes cellulose and pectin-degrading enzymes, as studied on apple fruits (Kim et al., 2001). In further studies, it may thus be interesting to investigate the effect of *B. dothidea* Fus3 on the expression of genes encoding cellulases and pectinases. The pathogenicity defect of Δ*Cgmk1* mutants of *C. gloeosporioides* is not exclusively due to appressorium formation defects, as these mutants were likewise unable to cause disease on wounded plants (He et al., 2017). Likewise, the *FUS3*-related MAPK *Cf*Pmk1of *Colletotrichum fructicola*, a pathogen causing severe diseases on a wide range of host plants, is required for full radial growth rates, formation of aerial hyphae, hyphal melanization, appressorium differentiation and host tissue colonization even on wounded leaves (Liang et al., 2019). Histopathological studies have shown that *Alternaria* species differentiate non-melanized appressoria in order to infect their hosts (Dita et al., 2007). The role of *FUS3* homologs in *Alternaria* species is of particular interest, as the MAP kinases of these pathogens are most closely related to the corresponding enzyme of *B. dothidea*. Strikingly, the MAPK gene of the citrus pathogen *A. alternata*, *AaFUS3*, is necessary for conidial development (Lin et al., 2010). Similarly, Infection symptom was not observed on the host plant inoculated with *Fus3* homologues gene deleted fungal strain such as *Cpmk1* of *Claviceps purpurea*, *PfFus3* of *Pseudocercospora fijiensis*, *fmk1* of *Fusarium oxysporum*, *FvMK1* of *Fusarium verticillioides*, *MAP1* of *Fusarium graminearum*, and

BMP1 of *Botrytis cinerea* (Mey et al., 2002; Onyilo et al., 2018; Di Pietro et al., 2001; Ortoneda et al., 2004; Zhang et al., 2011; Urban et al., 2003; Zheng et al., 2000). Likewise, *B. dothidea* Δ*fus3* mutants were completely conidiation incompetent, suggesting that defects in *FUS3* would lead to failure in disease spreading. Indeed, both ascospores and conidia of the ascomycete pathogen *Microcyclus ulei* have been shown to play a striking role in in the initiation and spread of South American leaf blight disease in a rubber tree plantation (Guyot et al., 2014). Similarly, Mutant deleted with *CfMK1* of *Colletotrichum fructicola*, *Gpmk1* of *Fusarium graminearum*, *VMK1* of *Verticillium dahlia* or gene homologous with *Fus3* of *Bipolaris oryzae* could not or less produce conidia on solid media (Li et al., 2022; Moriwaki et al., 2007; Jenczmionka et al., 2003; Rauyaree et al., 2005). Also, Pycnidia of *Mycosphaerella graminicola*, in which *MgFus3,* orthologous MAPK *Fus3*, was deleted, was not formed *in vitro* test (Cousin et al., 2006) and this is likely true of the spread of numerous to ripe rot of kiwifruit. *AaFUS3* of *A. alternata* is also required for infection of intact, but dispensable for infection of wounded leaves (Lin et al., 2010). The fact that *AaFUS3* is required for melanization is also of interest (Lin et al., 2010), as Δ*fus3* mutants of *B. dothidea* likewise fail to synthesize pigments on OMA. Mycelium of *B. dothidea* was known being melanized in cultures (Dong and Guo, 2020; Sanchez-Hernández et al., 2002), suggesting Fus3 might related to melanin pigment formation. The role of pigmentation in the latter fungus remains to be elucidated, possibly by targeted deletion of a melanin biosynthesis pathway gene (Kubo, 1986). Also the Fus3-related MAP kinase Amk1 of *Alternaria brassicicola*, which is also similar to Fus3 of *B. dothidea*, is required for pathogenicity, likely by regulating the expression of genes encoding hydrolytic enzymes (Cho et al., 2007).

Our studies have shown that hyphae of Δ*fus3* mutants of *B. dothidea* formed on the kiwifruit surface were significantly thinner that WT hyphae, suggesting that *FUS3* may be involved in hyphal morphogenesis. Moreover, structures reminiscent of hyphopodia were

well-developed in the WT strain, but were distorted in the mutants. Interestingly, hyphae of the *Neurospora crassa* Δ*mak-2* as well as of the *Cytospora chrysosperma* Δ*Ccpmk1* mutants, both mutated genes are *FUS3* homologs, were thinner as compared to those of the corresponding WT strains (Pandey et al., 2004; Yu et al., 2019). Misshapen or malformed hyphae may result from insufficient adhesion to the underlying surface, which may be due to a lack of hydrophobin formation. Indeed, *FUS3*-like MAP kinases have been shown to control hydrophobin formation (Talbot et al., 1993; Di Pietro et al., 2001; Zhang et al., 2010). Occasionally, hyphae of *B. dothidea* were not properly adhering to the kiwifruit surface, as observed by SEM in Δ*fus3* mutants, and it would be interesting to investigate whether genes involved in the formation of hydrophobins or other adhesive materials are affected by deletion of *FUS3* in the kiwi pathogen.

In this paper we have identified *FUS3* as a new pathogenicity factor of *B. dothidea*. Δ*fus3* mutants are unable to differentiate functional hyphae on the fruit surface at pre-penetration stages, are unable to invade the host and to cause ripe rot. This discovery may help to develop disease control strategies employing *FUS3* transcripts or the Fus3 protein as a target for SIGS or fungicide applications.

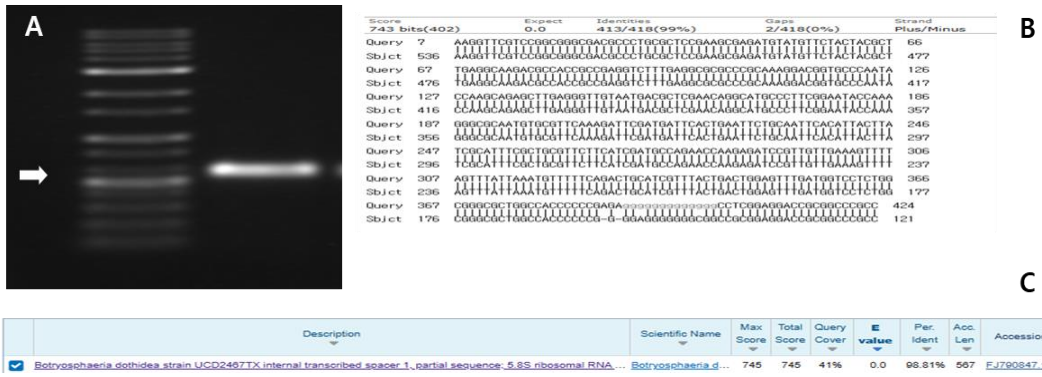

Supplemental Fig. 1. Molecular analysis of fungal isolates from infected kiwifruit shown ripe rot symptom. Electrophoresis image of amplified fungal DNA from the infected kiwi fruit using ITS1 and ITS4 primers (A), comparison of sequence between the fungal isolate and *Botryosphaeria dothidea* in NCBI (B), blast result (C). The arrow indicates 600bp.

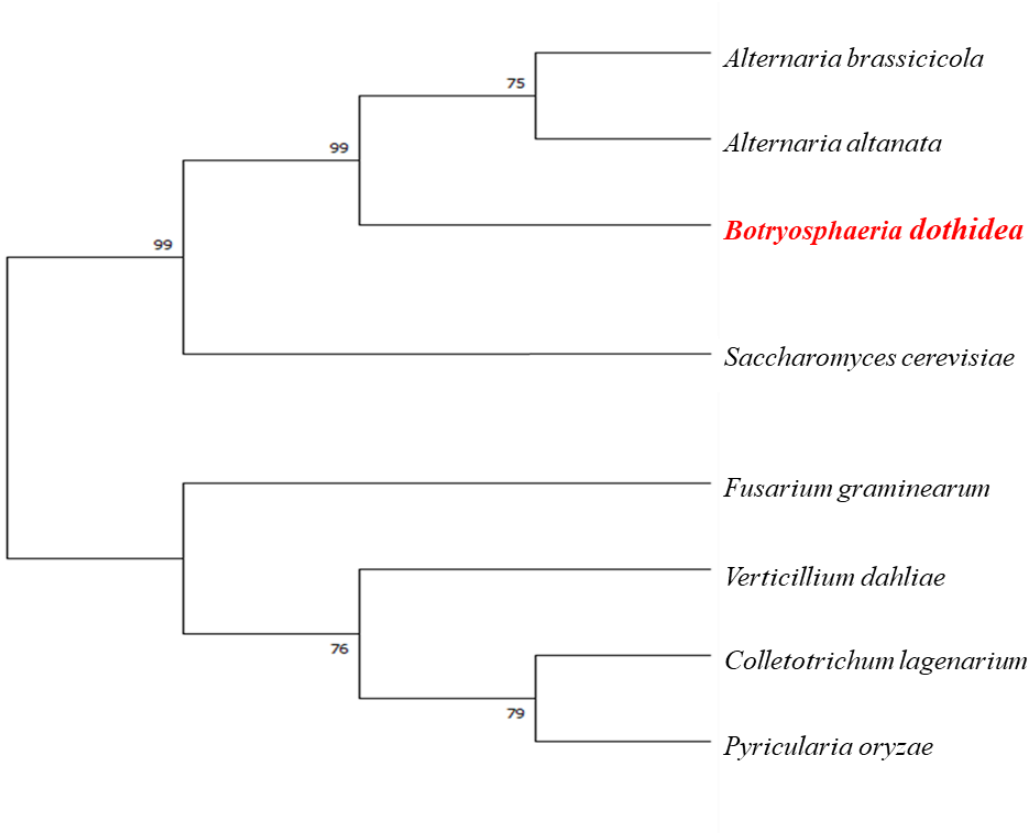

Supplemental Fig. 2. Phylogenetic tree of Fus3 related proteins from filamentous ascomycete pathogens, including *Botryosphaeria dothidea*, and from the model yeast *Saccharomyces cerevisiae*. Genetic information was acquired from NCBI site. The each number on branch represents the percentage in bootstrap 1,000 replicates..

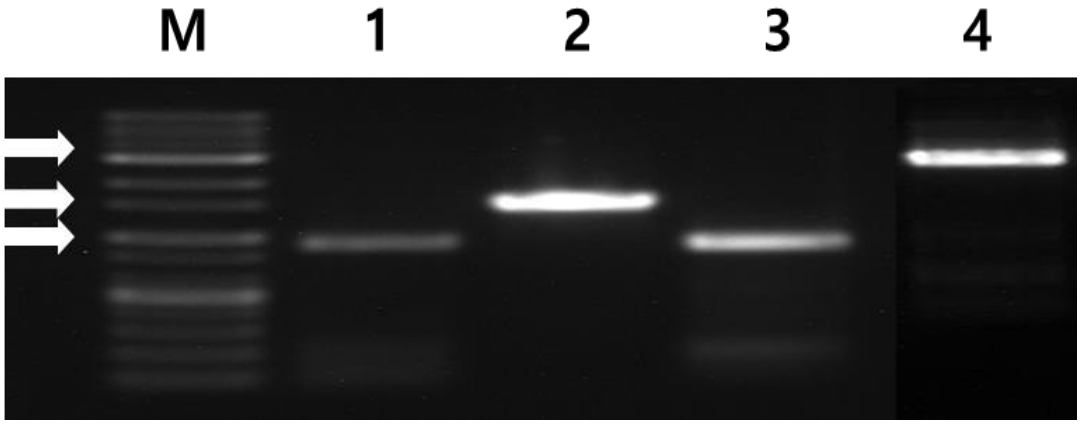

Supplemental Fig. 3. Gel electrophoresis images of PCR products. M: 1-kb DNA ladder (BIOFACT, Co. Ltd.) Lanes 1: Left flank, 2: Nourseothricin resistance gene, 3: Right flank, 4: Nested PCR product. Arrows indicate 3.4, 1.4 and 1.0 kb, respectively.

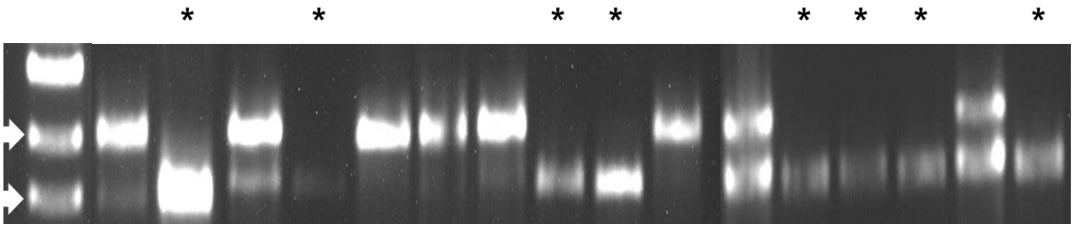

Supplemental Fig. 4. Gel electrophoresis image of PCR screening amplified with primer sets NBDOCheck-F/NBDOCheck-R for checking target gene (2.0 kb) deleted and cassettes gene inserted (1.5 kb). Accent marker indicates target gene deleted mutants. The arrow indicates 1.5 and 2.0 kb.

Supplemental table 1. Primer information to amplify PCR products for transformation.

Name	Target gene	Sequence (5' -> '3)
NBDOLF-F	Left flank	TGCGACGCATGTCAAACAC
NBDOLF-R		GACCAATCCGGCCCGAATCAGCAGGGATCAACCAAGAG
NBDORF-F	Right flank	GTTGAGAATCGTTTCATCGGTTTTGGCGGTGAATGTGAACG
NBDORF-R		TTCTCGTGCGCTGTAGAGAC
Nourseo-F	Nourseothricin resistance gene	ATTCGGGCCGGATTGGTC
Nourseo-R		ACCGATGAAACGATTCTCAAC
NBDONes-F	Nested PCR	TTCAGGCGCGGCCCTATATG
NBDONes-R		TCCATGCTCGCCACCATACC
NBDOCheck-F	Mutation check	CCGCTCCAAATCTTCACCAC
NBDOCheck-R		TGCGCTCAATTGGTCTTCAC
ITS1	Internal transcribed space	TCCGTAGGTGAACCTGCGG
ITS4		TCCTCCGCTTATTGATATGC

Supplemental table 2. Summary of transformation efficiencies and generation of knock-out mutants in *Botryosphaeria dothidea* strain target mitogen activated protein kinase *Fus3* gene.

Target gene	Size (bp)	No. of transformants on regeneration media	No. of positive candidates by PCR screening	Percentage of positive candidates in PCR screening (%)	No. of knock out mutants on southern blot
Fus3	2,026	38	8	21	4

Ⅴ. 적　　요

자낭균에 속하는 *Botryosphaeria dothide* 는 키위 저장병의 원인균이며, 포자의 생산 및 감염균사의 분화가 과실을 직접 감염하는데 요구된다. 여러 곰팡이 병원균에서, *Saccharomyces cerevisiae* 의 mitogen activated protein kinase(MAPK) *Fus3* 유전자와 유사유전자가 감염구조 형성 및 병원성에 요구된다. *B. dothidea* 에서 *Fus3* 유전자의 역할을 밝히기 위하여, *Fus3* 유사유전자를 삭제하고 Δ*fus3* 변이체를 생성하였다. 인공배지에서, Δ*fus3* 균주의 강한 생장 저해가 관찰되었고, 균사는 검정색소 생성 능력이 현저히 감소하였다. 또한, 병원성 확인 실험에서, Δ*fus3* 균주가 접종된 키위 과실에서는 병징을 나타내지 않았고, 상처 접종한 키위 과실도 감염시키지 않았다. 주사전자현미경 결과에서는, 야생형 균주에서 두꺼운 균사를 형성하고 키위과실 표면에 빽빽하게 부착되어있었다. 이와는 반대로, Δ*fus3* 균주의 균사는 야생형균주 보다 얇고 키위의 표면에 단단히 부착되지 못하였다. 이러한 결과는 *B. dothidea* 에서 *Fus3* 유사유전자가 무성포자 형성, 균사 감염을 위한 부착, 그리고 키위과실의 병원성에 있어서 중요한 역할을 하는 것으로 보인다.

VI. REFERENCES

Aamir, S., Sutar, S., Singh, S. K. and Baghela, A. 2015. A rapid and efficient method of fungal genomic DNA extraction, suitable for PCR based molecular methods. *Plant Pathol. Quar*. 5: 74-81.

Baranwal, S., Azad, G. K., Singh, V. and Tomar, R. S. 2014. Signaling of chloroquine-induced stress in the yeast *Saccharomyces cerevisiae* requires the Hog1 and Slt2 mitogen-activated protein kinase pathways. *Antimicrob Agents Chemother*, 58(9):5552-5566.

Chen, R. E. and Thorner, J. 2007. Function and regulation in MAPK signaling pathways: lessons learned from the yeast *Saccharomyces cerevisiae*. *Biochim Biophys Acta Mol Cell Res*, 1773(8):1311-1340.

Chen, W., Kastner, C., Nowara, D., Oliveira-Garcia, E., Rutten, T., Zhao, Y., Deising, HB., Kumlehn, J. and Schweizer P. 2016. Host-induced silencing of *Fusarium culmorum* genes protects wheat from infection. *J. Exp. Bot*. 67:4979-4991.

Cho, Y., Cramer Jr, R. A., Kim, K. H., Davis, J., Mitchell, T. K., Figuli, P., Pryor, B. M., Lemasters, E. and Lawrence, C. B. 2007. The Fus3/Kss1 MAP kinase homolog *Amk1* regulates the expression of genes encoding hydrolytic enzymes in *Alternaria brassicicola*. *Fungal Genet Biol*, 44(6):543-553.

Chomczynski, P. 1992. One-hour downward alkaline capillary transfer for blotting of DNA and RNA. *Anal Biochem*, 201(1):134-139.

Cousin, A., Mehrabi, R., Guilleroux, M., Dufresne, M., Van der Lee, T., Waalwijk, C., Langin, T. and Kema, G. H. 2006. The MAP kinase-encoding gene *MgFus3* of the non-appressorium phytopathogen *Mycosphaerella graminicola* is required for penetration and in vitro pycnidia formation. *Mol Plant Pathol*, *7*(4):269-278.

Dai, Y., Wang, Z., Leng, J., Sui, Y., Jiang, M., Wisniewski, M., Liu, J. and Wang, Q. 2022. Eco-friendly management of postharvest fungal decays in kiwifruit. *Crit Rev Food Sci Nutr*, 62(30):8307-8318.

Deising HB, Gase I. and Kubo Y. 2017. The unpredictable risk imposed by microbial secondary metabolites: How safe is biological control of plant diseases? *J. Plant Dis. Prot*, 124:413-419.

Di Francesco, A., Martini, C. and Mari, M. 2016. Biological control of postharvest diseases

by microbial antagonists: how many mechanisms of action? *Eur J Plant Patho*, 145:711-717.

Di Pietro, A., García-Maceira, F. I., Méglecz, E. and Roncero, M. I. G. 2001. A MAP kinase of the vascular wilt fungus *Fusarium oxysporum* is essential for root penetration and pathogenesis. *Mol Microbiol*, 39(5):1140-1152..

Dita, M.A., Brommonschenkel, S.H. Matsuoka, K. and Matsuoka, E.S.G. 2007. Histopathological study of the *Alternaria solani* infection process in potato cultivars with different levels of early blight resistance. *J. Phytopathol*. 155:462-469.

Dong, B. Z. and Guo, L. Y. 2020. An efficient gene disruption method for the woody plant pathogen *Botryosphaeria dothidea*. *BMC Biotechnol*, 20:1-9.

Fan, Y., Liu, K., Lu, R., Gao, J., Song, W., Zhu, H., Tang, X., Liu, Y. and Miao, M. 2023. Cell-free supernatant of Bacillus subtilis reduces kiwifruit rot caused *by Botryosphaeria dothidea* through inducing oxidative stress in the pathogen. *J Fungi (Basel)*, 9(1):127.

Guyot, J., Condina, V., Doaré, F., Cilas, C.and, Sache, I. 2014. Role of ascospores and conidia in the initiation and spread of South American leaf blight in a rubber tree plantation. *Plant Pathol*, 63(3):510-518.

Hamel, L. P., Nicole, M. C., Duplessis, S. and Ellis, B. E. 2012. Mitogen-activated protein

kinase signaling in plant-interacting fungi: distinct messages from conserved messengers. *Plant Cell*, 24(4):1327-1351.

He, P., Wang, Y., Wang, X., Zhang, X. and Tian, C. 2017. The mitogen-activated protein kinase *CgMK1* governs appressorium formation, melanin synthesis, and plant infection of *Colletotrichum gloeosporioides*. *Front Microbiol*, 8:2216.

Jenczmionka, N. J., Maier, F. J., Lösch, A. P. and Schäfer, W. 2003. Mating, conidiation and pathogenicity of *Fusarium graminearum*, the main causal agent of the head-blight disease of wheat, are regulated by the MAP kinase gpmk1. *Curr Genet*, 43:87-95.

Kim, K. W., Park, E. W., Kim, Y. H., Ahn, K.-K., Kim, P. G., & Kim, K. S. (2001). Latency- and defense-related ultrastructural characteristics of apple fruit tissues infected with *Botryosphaeria dothidea*. *Phytopathology*, 91:165-172.

Koch A., Biedenkopf D., Furch A., Weber L., Rossbach O., Abdellatef E., Linicus L., Johannsmeier J., Jelonek L., Goesmann A., Cardoza V., McMillan J., Mentzel T. and Kogel K.H. 2016. An RNAi-based control of *Fusarium graminearum* infections through spraying of long dsRNAs involves a plant passage and is controlled by the fungal silencing machinery. *PLoS Pathog*, 12:e1005901.

Koch A., Biedenkopf D., Furch A., Weber L., Rossbach O., Abdellatef E., Linicus L.,

Johannsmeier J., Jelonek L., Goesmann A., Cardoza V., McMillan J., Mentzel T. and Kogel K.H. 2017. An RNAi-based control of *Fusarium graminearum* infections through spraying of long dsRNAs. In: Deising HB, Fraaije B, Mehl A, Oerke EC, Sierotzki H, Stammler G, Modern Fungicides and Antifungal Compounds. *DPG Verlag, Braunschweig*, pp 63-66.

Koh, Y. J., Hur, J. S., & Jung, J. S. 2005. Postharvest fruit rots of kiwifruit (*Actinidia deliciosa*) in Korea. *N Z J Crop Hortic Sci*, 33(3):303-310.

Kim, G. H. and Koh, Y. J. 2015. Control of postharvest fruit rot diseases of kiwifruit by antagonistic bacterium *Bacillus subtilis*. *Acta Hortic*,1096:377-382.

Kubo, Y. 1986. Melanin biosynthesis in fungi. *Trans. Mycol. Soc. Japan*, 27:487-500.

Ledesma, M., Shin, Y. H., Whiteman, S., Tyson, J., Kim, G. H., Hong, J. K., Birgit, Z. and Jeun, Y. C. 2021. Causal fungus of side rot on ‘Zesy002’ kiwifruit in Jeju Island, South Korea. *Res. Plant Dis*, 27(1):24-31.

Li, C., Sun, W., Cao, S., Hou, R., Li, X., Ming, L., Kan, J., Zhao, Y. and Liu, F. 2022. The *CfMK1* gene regulates reproduction, appressorium formation, and pathogenesis in a pear anthracnose-causing fungus. *J Fungi (Basel)*, 8(1):77.

Liang, X., Wei, T., Cao, M., Zhang, X., Liu, W., Kong, Y., Zhang, R. and Sun, G. 2019. The

MAP kinase *CfPMK1* is a key regulator of pathogenesis, development, and stress tolerance of *Colletotrichum fructicola*. *Front Microbiol,* 10:1070.

Lin, C. H., Yang, S. L., Wang, N. Y. and Chung, K. R. 2010. The FUS3 MAPK signaling pathway of the citrus pathogen *Alternaria alternata* functions independently or cooperatively with the fungal redox-responsive AP1 regulator for diverse developmental, physiological and pathogenic processes. *Fungal Genet Biol,* 47(4):381-391.

Ma, L., Li, X., Xing, F., Ma, J., Ma, X. and Jiang, Y. 2022. Fus3, as a critical kinase in MAPK cascade, regulates aflatoxin biosynthesis by controlling the substrate supply in *Aspergillus flavus*, rather than the cluster genes modulation. *Microbiol Spectr*, 10(1): e01269-21.

Madhani, H. D. and Fink, G. R. 1998. The control of filamentous differentiation and virulence in fungi. *Trends Cell Biol*, 8(9):348-353.

Malonek S., Rojas M. C., Hedden P., Gaskin P., Hopkins P., & Tudzynski B. (2004). The NADPH-cytochrome P450 reductase gene from *Gibberella fujikuroi* is essential for gibberellin biosynthesis. *J. Biol. Chem*, 279: 25075-25084.

Marsberg, A., Kemler, M., Jami, F., Nagel, J. H., Postma-Smidt, A., Naidoo, S., Wingfield, M. J., Crous, P. W., Spatafora, J. W., Hesee, C. N., Robbertse, B. and Slippers, B. 2017.

Botryosphaeria dothidea: a latent pathogen of global importance to woody plant health. *Mol Plant Pathol*, 18(4):477-488.

Martín, H., Rodríguez-Pachón, J. M., Ruiz, C., Nombela, C. and Molina, M. 2000. Regulatory mechanisms for modulation of signaling through the cell integrity Slt2-mediated pathway in *Saccharomyces cerevisiae*. *J Biol Chem*, 275(2):1511-1519.

McRae, A.G., Taneja1, J., Yee, K., Shi1, X., Haridas, S., LaButti, K., Singan, V., Grigoriev, I. V., & Wildermuth, M. C. (2023). Spray-induced gene silencing to identify powdery mildew gene targets and processes for powdery mildew control. *Mol. Plant Pathol*, 24: 1168-1183.

Mey, G., Oeser, B., Lebrun, M. H. and Tudzynski, P. 2002. The biotrophic, non-appressorium-forming grass pathogen *Claviceps purpurea* needs a *Fus3/Pmk1* homologous mitogen-activated protein kinase for colonization of rye ovarian tissue. *Mol Plant Microbe Interact*, 15(4):303-312.

Michailides, T. J., Morgan, D. P. and Felts, D. 1998. Spread of *Botryosphaeria dothidea* in central California pistachio orchards. *Acta Hort*, 470:582-591.

Mizuno, T., Masuda, Y. and Irie, K. 2015. The *Saccharomyces cerevisiae* AMPK, Snf1, negatively regulates the Hog1 MAPK pathway in ER stress response. *PLoS Genet*,

11(9):e1005491.

Moriwaki, A., Kihara, J., Mori, C. and Arase, S. 2007. A MAP kinase gene, *BMK1*, is required for conidiation and pathogenicity in the rice leaf spot pathogen *Bipolaris oryzae*. *Microbiol Res*, 162(2):108-114.

Nowara D, Gay A, Lacomme C, Shaw J, Ridout C, Douchkov D, Hensel G, Kumlehn J, Schweizer P (2010) HIGS: Host-induced gene silencing in the obligate biotrophic fungal pathogen *Blumeria graminis*. *Plant Cell*, 22: 3130-3141.

Oh, S. O., Kim, J. A., Jeon, H. S., Park, J. C., Koh, Y. J., Hur, H. and Hur, J. S. 2008. Antifungal activity of eucalyptus-derived phenolics against postharvest pathogens of kiwifruits. *Plant Pathol J*, 24(3):322-327.

Oliveira-Garcia E, von Tiedemann A. and Deising HB. 2021. The measure mix matters: multiple-component plant protection is indispensable for coping with the enormous genome plasticity and mutation rates in pathogenic microorganisms. *J. Plant Dis. Prot*, 128:3-6.

Onyilo, F., Tusiime, G., Tripathi, J. N., Chen, L. H., Falk, B., Stergiopoulos, I., Tushemereirwe, W., Kubiriba, J. and Tripathi, L. 2018. Silencing of the mitogen-activated protein kinases (MAPK) *Fus3* and *Slt2* in *Pseudocercospora fijiensis* reduces

growth and virulence on host plants. *Front Plant Sci*, 9:291.

Ortoneda, M., Guarro, J., Madrid, M. P., Caracuel, Z., Roncero, M. I. G., Mayayo, E. and Di Pietro, A. 2004. *Fusarium oxysporum* as a multihost model for the genetic dissection of fungal virulence in plants and mammals. *Infect Immun*, 72(3):1760-1766.

Pan, L., Zhao, X., Chen, M., Fu, Y., Xiang, M. and Chen, J. 2020. Effect of exogenous methyl jasmonate treatment on disease resistance of postharvest kiwifruit. *Food Chem*, 305:125483.

Pandey, A., Roca, M. G., Read, N. D. and Glass, N. L. 2004. Role of a mitogen-activated protein kinase pathway during conidial germination and hyphal fusion in *Neurospora crassa*. *Eukaryot. Cell*, 3(2):348-358.

Pang, L., Xia, B., Liu, X., Yi, Y., Jiang, L., Chen, C., Li, P., Zhang, M., Deng, X. and Wang, R. 2021. Improvement of antifungal activity of a culture filtrate of endophytic *Bacillus amyloliquefaciens* isolated from kiwifruit and its effect on postharvest quality of kiwifruit. *J Food Biochem*, 45(1): e13551.

Qiao, L., Lan, C., Capriotti, L., Ah-Fong, A., Sanchez, J.N., Hamby, R., Heller, J., Zhao, H., Glass, N.L., Judelson, H.S., Mezzetti, B., Niu, D. and Jin, H. 2021. Spray-induced gene silencing for disease control is dependent on the efficiency of pathogen RNA uptake.

Plant Biotechnol. J, 19:1756–1768.

Rauyaree, P., Ospina-Giraldo, M. D., Kang, S., Bhat, R. G., Subbarao, K. V., Grant, S. J., and Dobinson, K. F. 2005. Mutations in *VMK1*, a mitogen-activated protein kinase gene, affect microsclerotia formation and pathogenicity in *Verticillium dahliae*. *Curr Genet*, 48:109-116.

Rodriguez-Iglesias, A. and Schmoll, M. 2015. Protoplast transformation for genome manipulation in fungi. *Genetic Transformation Systems in Fungi, Vol. 1*, pp:21-40.

Sánchez-Hernández, M. E., Gutiérrez-García, J. and Trapero-Casas, A. 2002. *Botryosphaeria* canker of Cistus ladanifer. *Plant Pathol*, 51(3):365-373.

Sarkar A., & Roy-Barman, S. (2021) Spray-Induced Silencing of Pathogenicity Gene MoDES1 via Exogenous Double-Stranded RNA Can Confer Partial Resistance Against Fungal Blast in Rice. *Front. Plant Sci*, 12:733129.

Sumita, T., Izumitsu, K., Shigeyoshi, S., Gotoh, S., Yoshida, H., Tsuji, K., Yoshida, H., Kitade, Y. and Tanaka, C. 2019. An adaptor protein BmSte50 interacts with BmSte11 MAPKKK and is involved in host infection, conidiation, melanization, and sexual development in *Bipolaris maydis*. *Mycoscience*, 61(2):85-94.

Takano, Y., Kikuchi, T., Kubo, Y., Hamer, J. E., Mise, K. and Furusawa, I. 2000. The

Colletotrichum lagenarium MAP kinase gene *CMK1* regulates diverse aspects of fungal pathogenesis. *Mol Plant Microbe Interact*, 13(4):374-383.

Talbot, N. J., Ebbole, D. J. and Hamer, J. E. 1993. Identification and characterization of *MPG1*, a gene involved in pathogenicity from the rice blast fungus *Magnaporthe grisea*. *Plant Cell*, 5(11):1575-1590.

Taylor, J. W. and Berbee, M. L. 2006. Dating divergences in the Fungal Tree of Life: review and new analyses. *Mycologia*, 98(6):838-849.

Tsai, H. C., Yang, S. L. and Chung, K. R. 2013. Cyclic AMP-dependent protein kinase A negatively regulates conidia formation by the tangerine pathotype of *Alternaria alternata*. *World J Microbiol Biotechnol*, 29:289-300.

Turrà, D., Segorbe, D. and Di Pietro, A. 2014. Protein kinases in plant-pathogenic fungi: conserved regulators of infection. *Annu Rev Phytopathol*, 52:267-288.

Tyagi, S., Nanher, A. H., Sahay, S., Kumar, V., Bhamini, K., Nishad, S. K. and Ahmad, M. 2015. Kiwifruit: Health benefits and medicinal importance. *Rashtriya krishi*, 10(2):98-100.

Urban, M., Mott, E., Farley, T. and Hammond-Kosack, K. 2003. The *Fusarium graminearum MAP1* gene is essential for pathogenicity and development of perithecia. *Mol Plant*

Pathol, 4(5):347-359.

Wang, B., Liang, X., Hao, X., Dang, H., Hsiang, T., Gleason, M. L., Zhang, R. and Sun, G. 2021. Comparison of mitochondrial genomes provides insights into intron dynamics and evolution in *Botryosphaeria dothidea* and *B. kuwatsukai*. *Environ Microbiol*, 23(9):5320-5333.

Widmann, C., Gibson, S., Jarpe, M. B. and Johnson, G. L. 1999. Mitogen-activated protein kinase: conservation of a three-kinase module from yeast to human. *Physiol Rev*, 79(1):143-180.

Wu, Y., Xu, L., Liu, J., Yin, Z., Gao, X., Feng, H. and Huang, L. 2017. A mitogen-activated protein kinase gene (*VmPmk1*) regulates virulence and cell wall degrading enzyme expression in *Valsa mali*. *Microb Pathog*, 111:298-306.

Xiong, Q., Xu, J., Zhao, Y. and Wang, K. 2015. *CtPMK1*, a mitogen-activated-protein kinase gene, is required for conidiation, appressorium formation, and pathogenicity of *Colletotrichum truncatum* on soybean. *Ann Appl Biol*, 167(1):63-74.

Xu, J. R. and Hamer, J. E. 1996. MAP kinase and cAMP signaling regulate infection structure formation and pathogenic growth in the rice blast fungus *Magnaporthe grisea*. *Genes Dev*, 10(21):2696-2706.

Yu, L., Xiong, D., Han, Z., Liang, Y. and Tian, C. 2019. The mitogen-activated protein kinase gene *CcPmk1* is required for fungal growth, cell wall integrity and pathogenicity in *Cytospora chrysosperma*. *Fungal Genet Biol*, 128:1-13.

Yu, J. H., Hamari, Z., Han, K. H., Seo, J. A., Reyes-Domínguez, Y. and Scazzocchio, C. 2004. Double-joint PCR: a PCR-based molecular tool for gene manipulations in filamentous fungi. *Fungal Genet Biol*, 41(11):973-981.

Zhang, Y., Zhang, J., Jiang, X., Wang, G., Luo, Z., Fan, Y., Wu, Z. and Pei, Y. 2010. Requirement of a mitogen-activated protein kinase for appressorium formation and penetration of insect cuticle by the entomopathogenic fungus *Beauveria bassiana*. *Appl Environ Microbiol*, 76(7):2262-2270.

Zhang, Y., Choi, Y. E., Zou, X. and Xu, J. R. 2011. The *FvMK1* mitogen-activated protein kinase gene regulates conidiation, pathogenesis, and fumonisin production in *Fusarium verticillioides*. *Fungal Genet Biol*, 48(2):71-79.

Zhang, C., Long, Y., Li, J., Li, M., Xing, D., An, H., Wu, X. and Wu, Y. 2020. A chitosan composite film sprayed before pathogen infection effectively controls postharvest soft rot in kiwifruit. *Agronomy (Basel)*, 10(2):265.

Zheng, L., Campbell, M., Murphy, J., Lam, S. and Xu, J. R. 2000. The *BMP1* gene is

essential for pathogenicity in the gray mold fungus *Botrytis cinerea*. *Mol Plant Microbe Interact*, 13(7):724-732.

Part C. Chemical control of kiwifruit against ripe rot

List of Figures

List of tables

ABSTRACT

ripe rot caused by *B. dothidea* is one of the serious diseases in postharvest kiwifruits. In order to control the ripe rot on *A. chinensis* cultivar Gold3, several commercial fungicides were selected by antifungal test on an artificial medium. Furthermore, disease suppression by the selected fungicides was evaluated on the kiwifruits by inoculation with conidial suspension of *B. dothidea*. On the artificial medium Tebuconazole, Iprodione and Boscalid+Fludioxonil were shown the most effective antifungal activity. However, in the bio-test Pyraclostrobin+Boscalid and Iminoctadine-tris were the most effective agrichemicals on the kiwifruits. On the other hand, the infection structures of *B. dothidea* on kiwifruits treated with agrichemical Pyraclostrobin+Boscalid were observed with a fluorescent microscope. Most of conidia of the fungus were not germinated on the kiwifruit treated with the agrichemical whereas on the untreated fruit the fungal conidia were mostly germinated. Also, chemical residue of of Pyraclostrobin + Boscalid was measured lower than MRL standard in Korea until 1 month before harvest. Based on this observation it was suggested that the ripe rot may be suppressed through the inhibition of conidial germination on the kiwifruit treated with the agrichemical.

Key words: fluorescence microscopy, infection structure, plant protection, postharvest disease ripe rot

I. INTRODUCTION

During the storage of kiwifruit several diseases often occur during low temperature storage. In a study of postharvest rots of 'Hort16A' in New Zealand most of the rots were found to be caused by *Diaporthe* spp., *Botrytis cinerea*, or *Botryosphaeria dothidea* (Manning et al., 2003). A survey of Korean kiwifruit orchards in 1999 showed that as much as 32% of kiwifruit had soft rot caused by these diseases (Koh et al., 2003). Among these, *B. dothidea* was the main fungus causing postharvest diseases and accounted for 83.3% of the fungal pathogens (Koh et al., 2003).

In Korea, 20.5% of kiwifruit cultivar 'Hayward' (*Actinidia chinensis* var. *deliciosa*) was lost with ripe rot caused by *B. dothidea* in 2014 (Kim and Koh, 2018). Another cultivar of *A. chinensis* var. *deliciosa* (Gamrok) was known to be more susceptible to *B. dothidea* because of its higher sugar contents than other cultivars (Kim et al., 2017). To control postharvest rot on kiwifruit, many agrochemicals were tested in kiwifruit orchards, especially cultivating kiwifruit cultivar *A. chinensis* 'Gold3'.

In this study, in order to evaluate the relative efficacy of the currently used chemical products, the direct protection rate of the chemicals were evaluated by agar plate assays. To further optimize agrochemicals used on-orchard, agrochemicals which were shown to inhibit antifungal activity in the agar plate test were assayed for efficacy in a bio-test with 'Gold3' fruit. Furthermore, to reveal the disease suppression mechanism on kiwifruit by these chemicals, the infection structures of *B. dothidea* were observed using a fluorescence microscope. In addition, chemical residue was investigated before of field application directly for safety.

II. MATERIALS AND METHODS

1. Fruit material.

Kiwifruit (*Actinidia chinensis* var. *chinensis* cultivar 'Gold3') were supplied by Zespri Co. Ltd. in Jeju Korea. The kiwifruit were sterilized with 1% sodium hypochlorite, 70% ethyl alcohol each for 60 s and washed with sterilized water three times. After drying at room temperature the kiwifruit were used for inoculation.

2. Fungal inoculum

B. dothidea isolate C1.1 was isolated from 'Gold3' kiwifruit showing ripe rot symptom, which is visually similar to Ripe rot, from an orchard of Jeju Island Korea during the 2018 harvest season (Ledesma et al., 2021). This isolate was held in Jeju University plant pathology general culture collection at –80°C and used in this experiment. For sporulation, *B. dothidea* was grown on an oatmeal agar medium (Becton, Dickinson and Company, Claix, France) under aerobic conditions at 28℃ with 7,000 lux in daytime for 7 days. Mycelium of *B. dothidea* was scraped with a loop and incubated another 7 days under the same conditions. In the plate 10 ml of sterilized water was added and conidia were harvested with a brush. The conidial suspension was filtered with double folded Miracloth (Calbiochem, Darmstadt,

Germany). The concentration of inoculum was adjusted to 1×10^5 conidia/ml using a hemocytometer (Hausser Scientific Inc., Horsham, PA, USA) and used as inoculum.

3. Agrochemical evaluation

In vitro test.

The effect of several agrochemicals were tested in potato dextrose agar (PDA; Becton, Dickinson and Company) medium. All chemicals were added into the PDA at the recommended concentration for field application, respectively. Some of the agrochemicals were subsequently diluted because the inoculated fungi did not grow. The list of agrochemicals and recommended concentrations are given in Table 1. As the control, PDA without chemicals was used. Mycelium of *B. dothidea* (ø = 5 mm) was inoculated on the PDA medium added with the different agrochemicals and incubated at 25℃ for 7 days. The diameter of the colony was measured with a ruler. This experiment was replicated three times including three PDA plates each.

Table 1. Agrichemicals used and its applied concentration in the PDA medium

Mode of action	Ingredients	Applied concentration(ppm)	Diluted concentration(ppm)
QOI	Iminoctadine-tris	1,000	-*
	Azoxystrobin	1,000	-
	Trifloxystrobin	250	
	Fluopyram	250	-
SDHI	Iprodione	1,000	100
	Boscalid	500	-
SDHI+ 12	Boscalid-Fludioxonil	1,000	10
DMI	Tebuconazole	500	50
DMI+SDHI	Pyraclostrobin-Boscalid	500	-
MBC	Thiophanate methyl	1,000	-
9	Cyprodinil	500	-
29	Fluazinam	500	-

*not tested

***In vivo* test.**

Agrochemicals which revealed direct anti-fungal effect on agar plates such as iprodione, tebuconazole, boscalid-fludioxonil, fluazinam, iminoctadinetris, thiophanate methyl, trifloxystrobin, cyprodinil and pyraclostrobin + boscalid were used in this experiment. All chemicals were applied to 'Gold3' kiwifruit previously wounded with a sterile stick (ø = 0.5 mm) at the recommended concentration for field application. After drying at room temperature the treated fruit were used for fungal inoculation.

A drop of 70 μl of conidial suspension of *B. dothidea* with 0.01% Tween-20 was inoculated onto the wounded part of each kiwifruit. The inoculated fruit were placed in an incubator maintained at 28℃, 90% relative humidity, for 7 days. As a control, sterilized 0.01% Tween-20 solution was applied instead of the conidial suspension. The symptoms on the fruit were examined and the lesions were measured with a ruler. The experiments were separately replicated 3 times which contained six kiwifruit each treatment.

4. Observation with a fluorescence microscope

To investigate the infection behavior of *B. dothidea* kiwifruit treated with pyraclostrobin + boscalid was observed with a fluorescence microscope (BX60, Olympus, Tokyo, Japan). The kiwifruit surfaces were inoculated with 60 μl of *B. dothidea* conidial suspension and the inoculated parts were excised with a razor in size of 5 × 5 mm2 at 3, 6, and 12 h after inoculation. The peel tissues were fixed with 2% glutaraldehyde in sodium

phosphate buffer (pH 7.2) at 4℃ for 2 h. After fixation, the samples were washed with sodium phosphate buffer three times (10 min each) and dyed with 0.2% diethanol (UVtex-2B, Polysciences, Inc., Muellheim, Germany) for 30 m at room temperature. After washing with H_2O three times the samples were mounted on glass slides with 70% glycerin (glycerin, OCI Company Ltd., Seoul, Korea). Infected sites were observed with a fluorescent filter set (exciter filter, BP 400-440; interference beam splitter, FT 460; barrier filter, LP 470). The germinated conidia were counted and the length of hyphae was measured. Experiments were separately replicated three times using three samples for each treatment.

5. Scanning electron microscopy of the kiwifruit after fungal inoculation

Kiwifruit surfaces of ‘Gold3’ pre-treated with agrichemicals and then inoculated with *B. dothidea* were observed at 1, 2, and 3 days after inoculation using a scanning electron microscope (FE-SEM Mira3, Tescan Ltd., Brno, Czech Republic).

The inoculated kiwifruit were cut to 0.4 × 0.6 mm2 using a sterile blade. Fixation, dehydration and embedding of the fruit were performed according to Hayat (1989). The fruit samples were fixed in 2% (v/v) glutaraldehyde in 0.05 M phosphate buffer (pH 7.4) for 2 h. After washing with phosphate buffer for 10 min three times each, post fixation was performed in 2% (v/v) osmium tetroxide in phosphate buffer for 2 h at room temperature. After washing three times, the samples were dehydrated through an alcohol series (30%, 50%, 70%, 90%, and 100% two times for 30 min each). The samples were gently dried using a critical point drier (EM CPD 300, Leica, Jena, Germany). Samples were mounted on metallic stubs, gold-coated (~100 Å) with a sputter coater (Q150R Plus – Rotary Pumped Coater, Quorum Technologies Ltd., Sussex, UK) and viewed under the FE-SEM at 20 kV.

6. Test of chemical residue

To carry out chemical residue test, a chemical shown the most effective on the disease suppression *in vivo* test were selected as a candidate; pyraclostrobin + boscalid. Two orchards were tested for residue test and boundary was set as 1.5m for preventing splashes of the chemical to the other treatment. To determine the residue of chemicals, the chemicals were pre-treated on the kiwifruit at 1, 2, and 3 months before harvest the kiwifruit. 1L of chemical suspension at field concentration was sprayed on 20 fruits for each treatment. Total 20 fruits for each treatment were harvested for residue test and sent to chemical residue analysis company PCAM (Daejeon, Korea).

7. Statistical analysis.

Data of diameters of mycelia on the PDA for determining the efficacy of agrochemicals, disease severity on kiwifruit treated with agrochemicals, and hyphal lengths on surfaces of kiwifruit were analyzed with Duncan's multiple range test. Rate of conidial germination was analyzed using t-test. All statistical analyses were conducted using SAS program version 9.0 (SAS Institute Inc., Cary, NC, USA). Statistical significance was considered at $P < 0.05$.

III. RESULTS

1. Antifungal effect on PDA medium amended with agrochemicals.

Hyphal growth suppression of *B. dothidea* by 12 commercial agrochemicals was evaluated on PDA medium. At 7 days after inoculation, hyphal growth was inhibited on all of the agrochemical amended media compared with the untreated control (Fig. 1). Especially, mycelium of *B. dothidea* did not grown on PDA amended with tebuconazole, iprodione and boscalid + fludioxonil at field application concentration (data not shown). Even when tebuconazole or iprodione were diluted 10 times, the antifungal effect was high compared with other agrochemicals tested (Fig. 2). Above all, PDA treated with boscalid + fludioxonil diluted 100 times was shown to have the best suppression effect compared with other chemicals in the in vitro experiment (Fig. 2).

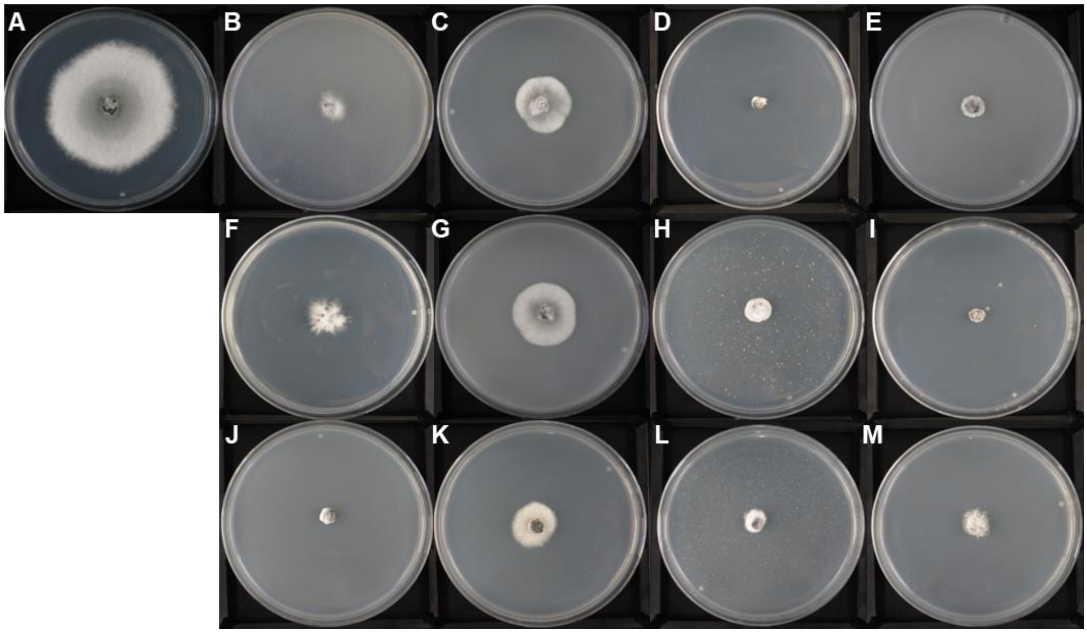

Fig. 1. Mycelium of *Botryosphaeria dothidea* grown on PDA medium added with different agrichemicals. The present photos were taken at 7 days after inoculation with the fungus. The recommended concentration for field application were added on the PDA medium, respectively. A, Control; B, Iminoctadine-tris; C, Azoxystrobin; D, Tebuconazole dilluted 10 times; E, Fluopyram+Thiophanate-methyl; F, Iprodione dilluted 10 times; G, Boscalid; H, Trifloxystrobin; I, Boscalid+Fludioxonil dilluted 100 times; J, Fluazinam; K, Fluopyram; L, Cyprodinil; M, Pyraclostrobin+Boscalid

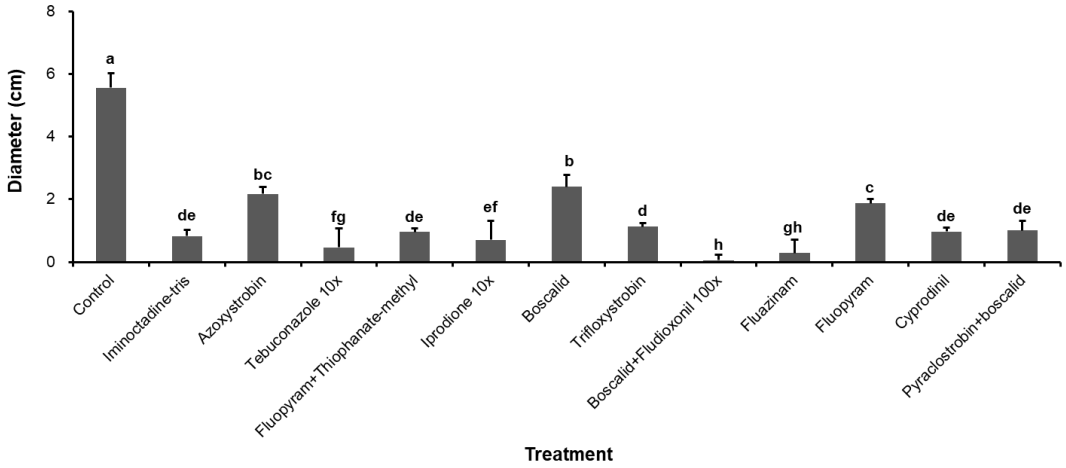

Fig. 2. Diameter of mycelium of *Botryosphaeria dothidea* grown on PDA medium added with different agrichemicals. The present photos were taken at 7 days after inoculation with the fungus. The recommended concentration for field application and were added on the PDA medium, respectively. Different letters on the columns indicate significant differences ($P < 0.05$) according to Duncan's multiple test.

2. Disease suppression on kiwifruit treated with agrochemicals.

To test the disease suppression effect on kiwifruit treated with the agrochemicals, *B. dothidea* was inoculated onto kiwifruit pre-treated with the most effective nine agrochemicals selected from the *in vitro* experiment. On untreated kiwifruit, symptoms of *B. dothidea* were visible at 3 days after inoculation. The lesion sizes were larger on the untreated fruit compared with all of the chemicals treated kiwifruit.

At 7 days after inoculation, the symptom diameter on all of the agrochemical pre-treated kiwifruit were reduced compared with those symptoms on the untreated control (Fig. 3). Especially, pyraclostrobin+boscalid and iminoctadine-tris were the most effective agrochemicals on kiwifruit, on which the disease suppression rates were 75% and 44% compared with the untreated control, respectively (Fig. 4). This indicates that the agrochemicals have a disease suppression effect on kiwifruit.

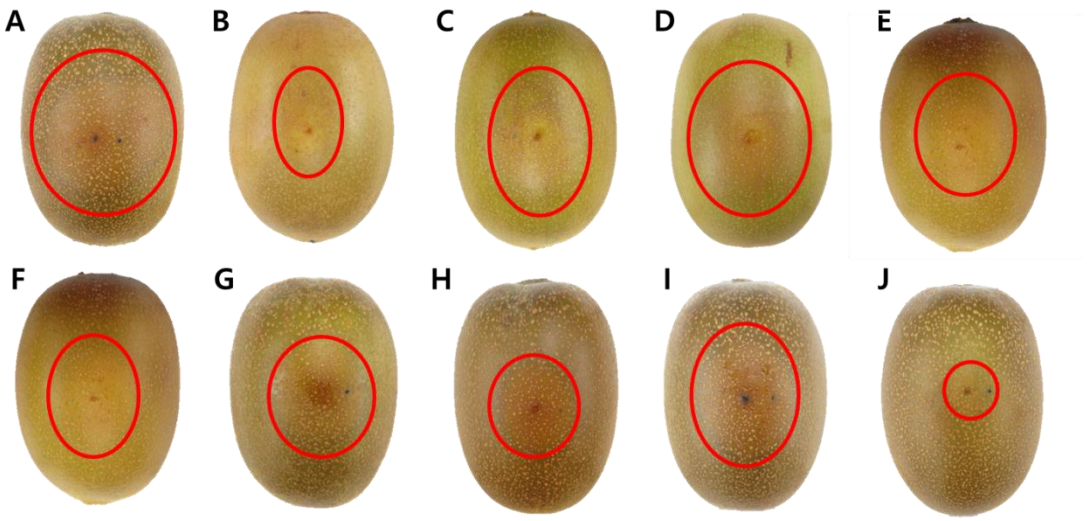

Fig. 3. Wounded Gold3 kiwifruit untreated (A), pre-treated with Iminoctadine-tris (B), Tebuconazole (C), Iprodione (D), Boscalid+fludioxonil (E), Fluazinam (F), Fluopyram+thiophanate-methyl (G), Trifloxystrobin (H), Cyprodinil (I), and Pyraclostrobin+Boscalid (J) which were inoculated with conidial suspension of *Botryosphaeria dothidea* and as a negative control both untreated/uninoculated kiwifruit (F). The recommended concentration for field application were pre-treated before fungal inoculation, respectively. The concentration of the conidial suspension of *B. dothidea* were 1 × 10^5 conidia/ml. The present photos were taken at 7 days after inoculation with the fungus. The circle indicates infected site.

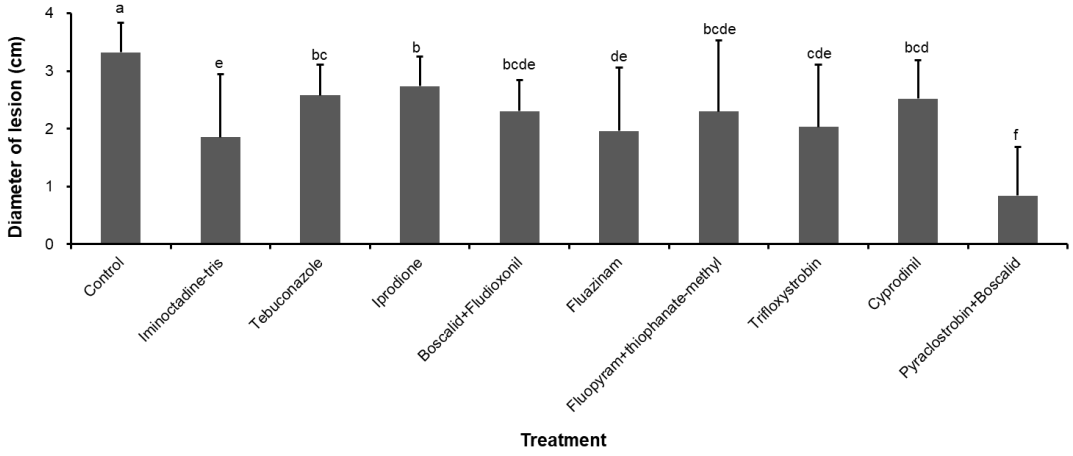

Fig. 4. Diameter of Ripe rot lesion on wounded Gold3 kiwi fruits treated with agrichemicals after inoculated with conidial suspension of *Botryosphaeria dothidea*. The recommended concentration for field application was pre-treated before fungal inoculation, respectively. The concentration of the conidial suspension of *B. dothidea* was 1×10^5 conidia/ml. The diameter of lesions was measured at 7 days after inoculation with the fungus. Different letters on the columns indicate significant differences ($P < 0.05$) according to Duncan's multiple test.

3. Fluorescent microscopy

To reveal the mechanism of disease suppression on kiwifruit treated with pyraclostrobin + boscalid, which was shown to be the most effective against *B. dothidea*, the infection structure of *B. dothidea* on kiwifruit were observed with a fluorescence microscope. At 3 h after inoculation some conidia were germinated on the untreated kiwifruit and 6 h later most conidia were germinated (Table 2). Hyphal growth developed rapidly and the surfaces of kiwifruit were covered with hyphae 12 h after inoculation (Fig. 5A-C). However, most conidia did not germinate on the agrochemical-treated kiwifruit during the whole observation period from 3 to 12 h after inoculation (Table 2, Fig. 5D-F). These observations indicated that the agrochemicals inhibited the conidial germination which might result in the suppression of disease severity. Even on kiwifruit treated with pyraclostrobin + boscalid 100 times diluted from field rates, most conidia had not germinated at 12 h after inoculation (data not shown), indicating that pyraclostrobin + boscalid was the most effective fungicide to suppress ripe rot on kiwifruit.

Table 2. Germination rate of *B. dothidea* on the surface of kiwifruit Gold3 untreated and treated with agrochemical Pyraclostrobin + Boscalid.

Treatment	Germination rate (%)		
	Hours after inoculation (h)		
	3	6	12
Untreated	13.7 ± 19.1[a]	72.5 ± 15.4	96.9 ± 2.1
Pyraclostrobin + Boscalid	0.0 ± 0.0	0.1 ± 0.3	0.0 ± 0.0
t-value	2.15	14.11	135.36
p-value	0.0476	<0.0001	<0.0001

[a] Mean ± standard deviation.

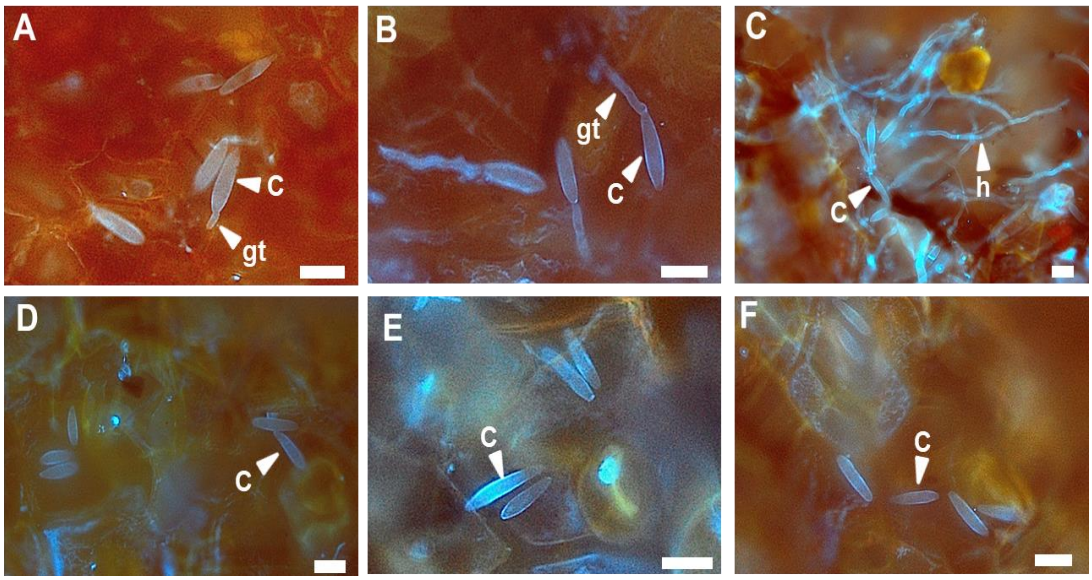

Fig. 5. Fluorescent microscopic observation of infection structures at 3, 6, 12 hours after inoculation on peels of kiwifruits untreated (A-C) and fungicide pyraclostrobin-boscalid(D-F). The concentration of fungicide and conidia suspension of *Botryosphaeria dothidea* were field application and 1 x 10^5 conidia/ml. Scale bars= 20 µm. c, conidium; h, hyphae; gt, gum tube.

4. Scanning electron microscopy

On the untreated kiwifruit, conidia of *B. dothidea* were morphologically intact and mostly germinated at 1 day after inoculation (Fig. 6A). One day later the hyphae of the fungus had grown on the surface of the kiwifruit and were extended widely at 3 days after inoculation (Fig. 6B and C). However, on the pyraclostrobin + boscalid pre-treated kiwifruit, some conidia of *B. dothidea* were morphologically changed (Fig. 6D, arrow) and most conidia had not germinated. The tapered conidia were often found at 2 days after inoculation (Fig. 6E, arrow) and most conidia still had not germinated. At 3 days after inoculation some hyphae were observed which were frequently branched (Fig. 6F, double arrows), indicating the fungicide may suppress the hyphal growth.

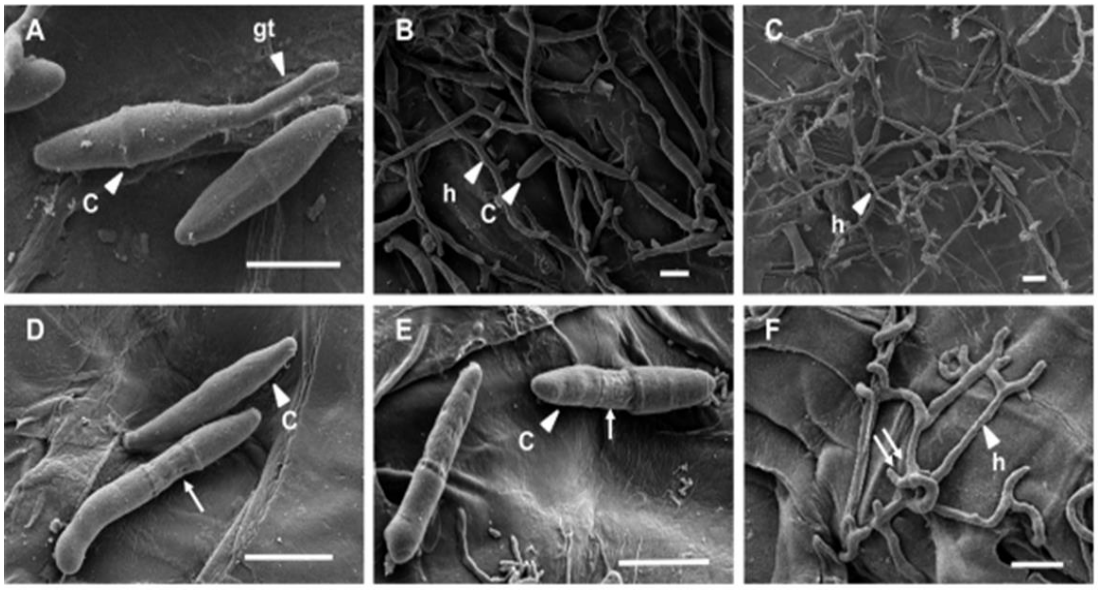

Fig. 6. Scanning electron microscopic observation of infection structures at 1, 2, and 3 days after inoculation on peels of kiwifruits untreated (A-C) and fungicide pyraclostrobin-boscalid (D-F). The concentration of fungicide and conidia suspension of *Botryosphaeria dothidea* were field application and 1×10^5 conidia/ml. Morphological change was observed on conidium (D and E, arrow) and branched hyphae (F, double arrows). Scale bars = 10 μm. c, conidium; h, hyphae; gt, gum tube.

5. Test of chemical residue

Both 2 chemicals pyraclostrobin and boscalid were detected in both orchards. Boscalid was detected on July to September in both orchards and much of the chemical residue was detected on September than July and August. However, boscalid was also detected on untreated fruit. In the pyraclostrobin applied case, no spray on August resulted in none residue of the chemical. However, the chemical was found on the fruit sprayed on July or September in both orchards (Table 3).

Table 3. Residue of chemicals on the kiwifruits sprayed with Pyraclostrobin, and Boscalid at the different times in two orchards

Number of orchard	Time of spray	Residue of chemical (ppm)	
		Pyraclostrobin (3mg/kg)**	Boscalid (5mg/kg)**
1	Control	0±0 b	0.69±0.26a*
	July	0.21±0.05 a	0.89±0.25 a
	Aug.	0±0 b	0.65±0.16 a
	Sept.	0.21±0.02 a	1.05±0.35 a
2	Control	0±0 c	0.06±0.02 c
	July	0.16±0.02 b	0.28±0.04 b
	Aug.	0±0 c	0.05±0.01 c
	Sept.	0.23±0.04 a	0.41±0.07 a

*The different letters on the table present significant (P< 0.05) difference according to Duncan's multiple test.

**Maximum residue limit (MRL) of chemicals compound on kiwifruit registered by Ministry of food and drug safety in Korea

IV. DISCUSSION

Although ripe rot caused by *B. dothidea* has been known in kiwifruit *A. chinensis* cultivars ‘Haegeum’ and ‘Hayward’, there was no report announcing ripe rot on the cultivar ‘Gold3’. Over the last decade the postharvest disease has often occurred on ‘Gold3’; this cultivar is known to be tolerant to Psa (Zespri International Limited, 2016). In a previous study, *B. dothidea* was isolated from symptomatic kiwifruit and confirmed as the causal fungus of ripe rot by fulfilling Koch's Postulates (Ledesma et al., 2021).

Protection efficacy of agrochemicals against ripe rot in cultivar ‘Hort16A’ and ‘Hayward’ has been previously reported. Among three agrochemicals tested, benomyl WP showed the highest efficacy, followed by thiophanatemethyl WP and carbendazim + diethofencarb WP when they were treated in the orchards Jeju Island, Korea (Kim et al., 2013).

In this study, among the agrochemicals tested boscalid + fludioxonil was shown to have the most effective antifungal activity in the artificial medium (Figs. 1 and 2). The efficacy of this chemical was so high that its concentration had to dilute as 100 fold in the in vitro experiment. However, in the bio-test on fruit, this mixture was not the most effective among the tested fungicides. Unexpectedly, pyraclostrobin + boscalid mixture was the most effective against ripe rot on ‘Gold3’ fruit (Fig. 4). It is not clearly explained why the efficacy of the agrochemicals was different between the in vitro and in vivo experiments. One of the reasons for this difference in efficacy could be that different inoculum types were used in each test (mycelium in the in vitro test and conidia in the in vivo test). It was also suggested that some factors such as fruit exudates or pH may influence the activity of the agrochemicals (Mihaylova-Kroumova et al., 2020; Zhao et al., 2016).

Boscalid is a pyridinecarboxamide which is active against a broad range of fungal pathogens including *Botrytis cinerea* causing grey mold (Veloukas and Karaoglanidis, 2012) or *Sclerotinia sclerotiorum* causing stem rot in canola (Munoz, 2016). Boscalid has been known as an inhibitor of succinate dehydrogenase which has a role in electron transport chain in mitochondria (Hatefi, 1985). Also, pyraclostrobin is a carbamate ester which is widely used as a fungicide for control of many plant pathogens such as *Alternaria* spp. (Survilienė and Dambrauskienė, 2006) or *Ascochyta rabiei* (Chang et al., 2007). This agrochemical inhibits energy transfer in mitochondria in the fugal cell (Sierotzki and Scalliet, 2013). Mixtures with pyraclostrobin and boscalid were effective against brown spot on the leaves of pear in orchards (Petré et al., 2015).

The infection behavior of *B. dothidea* in kiwifruit is not well known yet. In this study, it was observed that the conidia of *B. dothidea* germinate fast similar to some other fungal pathogens. Also, it seems the fungus can invade the host cells without forming appressoria (Fig. 5). In order to illustrate how the agrochemicals inhibit fungal infection, the infection structures were observed on the surface of kiwifruit 'Gold3' treated with pyraclostrobin + boscalid. On the agrochemical-treated kiwifruit there was a very low germination rate and restricted hyphal growth of *B. dothidea* (Table 2, Fig. 5). There have been previous reports that germination rates and hyphal development are decreased by this fungicide. Both germination rate and hyphal growth of *Alternaria alternata* and *Penicillium digitatum* were inhibited by boscalid treatment (Vega and Dewdney, 2015; Xu et al., 2020). Also, it was reported that the germination rate of *Puccinia striiformis* causing stripe rust in wheat (Kang et al., 2019) or *Colletotrichum acutatum* causing anthracnose in chili (Gao et al., 2017), was decreased by pyraclostrobin. Conidia and hyphae of *Monilinia fructicola* and *Botrytis cinerea* treated with mixtures of pyraclostrobin and boscalid did not germinate or develop well compared with untreated conidia and hyphae (Amiri et al., 2010; Kim and Xiao, 2010).

Electron microscopy of the fine structure of *B. dothidea* on the untreated kiwifruit showed the intact conidia and hyphae (Fig. 6A-C); this was similar to those observed with the fluorescence microscope (Fig. 5). Strangely, the fungal samples for SEM grew more slowly than those used for fluorescence microscopy; this was likely to be due to environmental differences during the incubation period such as temperature. Through the observation with SEM it was clearly shown that mixtures of pyraclostrobin and boscalid may suppress the growth of *B. dothidea* resulting in the morphological change of conidia and branch of hyphae. Similar observations were found on the kiwifruit pretreated with other fungicides such as iminoctadine-tris or fluazinam (data not shown).

In the chemical residue test, pyraclostrobin + boscalid could applicate until September, because the amount of chemical residues was detected less than those maximum residue level (MRL). Moreover, boscalid was detected on untreated fruits, suggesting potential splashing from neighboring treatments despite the presence of a buffer zone.

Therefore, it was suggested that the function of the agrochemicals in the suppression of ripe rot on kiwifruit may be the decreasing of germination rate and hyphal development of *B. dothidea*. Also, pyraclostrobin + boscalid were shown lower level above than MRL on the chemical residue test. However, for applying of agrochemicals to the fields, it would be necessary to undertake more experiments in order to prove their efficacy.

Ⅴ. 적　　요

키위 부패병은 *B. dothidea*에 의한 심각하게 피해를 주는 저장병중 하나이다. *A. chinensis* 의 Gold3 품종에서 키위부패병을 방제하기 위해 여러 농약을 선정하여 항진균실험을 인공배지에서 진행하였다. 더 나아가, 농약에의한 병억제정도를 키위 과실에 병원균 포자현탁액을 접종하여 평가하였다. 인공배지에서는, 테부코나졸, 이프로디온, 그리고 보스칼리드 플로디옥소닐 합제가 가장 효과가 좋은 것으로 보여졌다. 그러나, 생물실험에서는, 피라클로스트로빈 보스칼리드합제, 그리고 이미녹타딘트리스가 가장 효과가 좋은것으로 보여졌다. 또한, *B. dothidea*의 감염구조를 키위과실에 피라클로스트로빈 보스칼리드 합제를 처리하여 형광현미경으로 관찰하였다. 대부분의 포자가 농약을 처리한 과실에서 발아하지 못하였으며, 반면에 무처리 과실에서는 포자가 대부분 발아하였다. 또한, 잔류농약검사에서 피라클로스트로빈 보스칼리드 합제가 수확 한 달 전까지 한국에서의 MRL 기준보다 낮게 측정 되었다. 이 실험결과를 토대로, 농약을 처리하면 포자발아가 억제되어 키위 부패병이 감소하는 것으로 보여진다.

VI. REFERENCES

Amiri, A., Brannen, P. M. and Schnabel, G. 2010. Reduced sensitivity in *Monilinia fructicola* field isolates from South Carolina and Georgia to respiration inhibitor fungicides. *Plant Dis*, 94:737-743.

Chang, K. F., Ahmed, H. U., Hwang, S. F., Gossen, B. D., Strelkov, S. E., Blade, S. F. and Turnbull, G. D. 2007. Sensitivity of field populations of *Ascochyta rabiei* to chlorothalonil, mancozeb and pyraclostrobin fungicides and effect of strobilurin fungicides on the progress of ascochyta blight of chickpea. *Can. J. Plant Sci*, 87:937-944

Gao, Y.-Y., He, L.-F., Li, B.-X., Mu, W., Lin, J. and Liu, F. 2017. Sensitivity of *Colletotrichum acutatum* to six fungicides and reduction in incidence and severity of chili anthracnose using pyraclostrobin. *Australas. Plant Pathol*, 46:521-528.

Hatefi, Y. 1985. The mitochondrial electron transport and oxidative phosphorylation system. *Annu. Rev. Biochem*, 54:1015-1069.

Kang, Z., Li, X., Wan, A., Wang, M. and Chen, X. 2019. Differential sensitivity among *Puccinia striiformis* f. sp. *tritici* isolates to propiconazole and pyraclostrobin fungicides. *Can. J. Plant Pathol*, 41:415-434.

Kim, G. H. and Koh, Y. J. 2018. Incidence rates of major diseases on green-fleshed kiwifruit cv. hayward and yellow-fleshed kiwifruit cv. haegeum. *Res. Plant Dis*, 24:175-181.

Kim, G. H., Lee, Y. S., Jung, J. S., Hur, J.-S. and Koh, Y. J. 2013. Optimal spray time, interval and number of preventive fungicides for the control of fruit rots of green and gold kiwifruit cultivars. *Res. Plant Dis*, 19:1-6.

Kim, M.-J., Kwon, Y., Shin, M. H., Kim, J. G., Kwak, Y.-S. and Kwack, Y.-B. 2017. Fungal infection occurrence on new cultivars of kiwifruit correlated with fruit soluble solids content and firmness. *Korean J. Soil Sci. Fertil*, 50:215-225.

Kim, Y. K. and Xiao, C. L. 2010. Resistance to pyraclostrobin and boscalid in populations of *Botrytis cinerea* from stored Suppression Ripe Rot with Fungicides 355 apples in Washington State. *Plant Dis*, 94:604-612.

Koh, Y. J., Jung, J. S. and Hur, J. S. 2003. Current status of occurrence of major diseases on kiwifruits and their control in Korea. *Acta Hortic*, 610:437-443.

Ledesma, M., Shin, Y. H., Whiteman, S., Tyson, J., Kim, G. H., Hong, J. K., Birgit, Z. and Jeun, Y. C. 2021. Causal fungus of side rot on 'Zesy002' kiwifruit in Jeju Island, South Korea. *Res. Plant Dis*, 27(1):24-31.

Manning, M. A., Meier, X., Olsen, T. L. and Johnston, P. R. 2003. Fungi associated with fruit rots of *Actinidia chinensis* 'Hort16A' in New Zealand. *N. Z. J. Crop Hortic. Sci*, 31:315-324.

Mihaylova-Kroumova, A. B., Artiouchine, I., Korenkov, V. D. and Wagner, G. J. 2020. Patterns of inheritance of acylsugar acyl groups in selected interspecific hybrids of genus *Nicotiana*. *J. Plant Res*, 133:509-523.

Munoz, C. L. 2016. Sensitivity of *Sclerotinia sclerotiorum* isolates from North Central us to azoxystrobin and boscalid. M.S. thesis. North Dakota State University, Fargo, ND, USA.

Petré, R., Labourdette, G., Braun, C. A., Meredith, R., Hauke, K., Van Hemelrijck, W., Schoofs, H., Deckers, T., Keulemans, W., Schoevaerts, C., Becker, R. C. and De Maeyer, L. 2015. Fosetyl-al (Aliette®), a plant defense enhancer with good efficacy on bacteria and on ascomycetes in apples and pears. *Acta Hortic*, 1094:431-438.

Sierotzki, H. and Scalliet, G. 2013. A review of current knowledge of resistance aspects for the next-generation succinate dehydrogenase inhibitor fungicides. *Phytopathology*, 103:880- 887.

Survilienė, E. and Dambrauskienė, E. 2006. Effect of different active ingredients of fungicides on *Alternaria* spp. growth *in vitro*. *Agron. Res*, 4:403-406.

Vega, B. and Dewdney, M. M. 2015. Sensitivity of *Alternaria alternata* from citrus to boscalid and polymorphism in ironsulfur and in anchored membrane subunits of succinate dehydrogenase. *Plant Dis*, 99:231-239.

Veloukas, T. and Karaoglanidis, G. S. 2012. Biological activity of the succinate dehydrogenase inhibitor fluopyram against *Botrytis cinerea* and fungal baseline sensitivity. *Pest Manag*. Sci, 68:858-864.

X u, Q., Zhang, K., Fu, Y., Ma, H. and Zhu, F. 2020. Toxic action and baseline sensitivity of boscalid against *Penicillium digitatum*. *Crop Prot*, 137:105272.

Z espri International Limited. 2016. Zespri annual review 2015/16. Zespri International Limited., Mount Maunganui, New Zealand, 22 pp.

Zhao, L., Huang, Y., Hu, J., Zhou, H., Adeleye, A. S. and Keller, A. A. 2016. 1 H NMR and GC-MS based metabolomics reveal defense and detoxification mechanism of cucumber plant under nano-cu stress. *Environ. Sci. Technol*, 50:2000-2010